Technobius

A peer-reviewed open-access journal

Contacts: Website: https://technobius.kz/
E-mail: technobius.research@gmail.com

CONTENTS

Article

Age-dependent trends in compressive strength of concrete incorporating fly ash

Sungat Akhazhanov[1], Gulshat Tleulenova[2], Sabit Karaulov[3], Shyngys Zharassov[4,*], Alisher Mukhamejan[2]

[1]Department of Algebra, Mathematical Logic and Geometry named after T.G. Mustafin, Karaganda Buketov University, Karaganda, Kazakhstan
[2]Department of Civil Engineering, L.N. Gumilyov Eurasian National University, Astana, Kazakhstan
[3]Solid Research Group, LLP, Astana, Kazakhstan
[4]Research laboratory of applied mechanics and robotics, Karaganda Buketov University, Karaganda, Kazakhstan
*Correspondence: zhshzh95@gmail.com

Abstract. The research investigates the transformative potential of fly ash, an industrial byproduct, in enhancing concrete compressive strength and addressing environmental concerns associated with its disposal. The study employs a rich dataset from Mendeley Data, comprising 471 data points, to comprehensively explore the impact of fly ash on concrete strength at different ages. The analysis involves determining optimal compositions with fly ash, evaluating the fraction of cement replacement, and analyzing the generalized effect on compressive strength through graphical representation. Results reveal an inverse relationship between fly ash content and compressive strength, with nuanced patterns emerging at different curing ages. Despite the negative correlation, opportunities exist to optimize concrete formulations for specific strength requirements by judiciously incorporating fly ash. The weighted sum analysis identifies a composition with 33.6% replacement of binder by fly ash as optimal in the long term, showcasing the potential of this waste product as a valuable resource in sustainable concrete engineering.
Keywords: concrete, fly ash, compressive strength, curing age, weighted sum.

1. Introduction

The focus of concrete research has progressively shifted towards incorporating fly ash, a byproduct of combustion processes, into concrete mixtures [1]. Previously regarded as waste, fly ash has now gained significance not only for its ecological implications but also for its potential impact on concrete compressive strength [2].

The global construction industry, driven by a growing demand for concrete, has generated substantial amounts of industrial byproducts, including fly ash [3]. These byproducts, often dismissed as waste, hold untapped potential that researchers are eager to explore. Fly ash, with its pozzolanic properties, can significantly influence the mechanical and durability characteristics of concrete [4].

The problem at hand encompasses two aspects. Firstly, there is a pressing environmental concern related to the disposal of fly ash, which, if unaddressed, may lead to soil and water contamination [5]. Secondly, there is a compelling need to enhance the performance of concrete structures to meet modern construction demands [6]. The incorporation of fly ash into concrete formulations presents a unique opportunity to simultaneously address both challenges— transforming a potential environmental hazard into a valuable resource for the construction industry [7].

As we navigate this research landscape, our primary objective is to comprehensively investigate the impact of fly ash on the compressive strength of concrete at different ages. Concrete

strength is a critical parameter directly influencing the structural integrity and longevity of buildings and infrastructure [8]. By understanding how the inclusion of fly ash affects this fundamental property, we contribute to academic discourse and offer practical insights that can reshape approaches to concrete engineering. Our exploration relies on Mendeley Data, a repository rich with diverse compositions and corresponding compressive strength data [9]. This dataset allows us to delve into the nuances of various concrete formulations, each with its unique blend of cementitious materials and fly ash content. The inclusion of data from different ages provides a dynamic perspective, enabling us to track the evolution of concrete strength over time in the presence of fly ash.

This research aims to unravel the intricate relationship between fly ash and concrete strength, utilizing a rich dataset sourced from Mendeley Data.

2. Methods

The data for analysis was retrieved from [9]. The data comprises 471 tabular data points related to the compressive strength of concrete for various ages of curing (from 1 to 365 days), encompassing data from compositions that include fly ash.
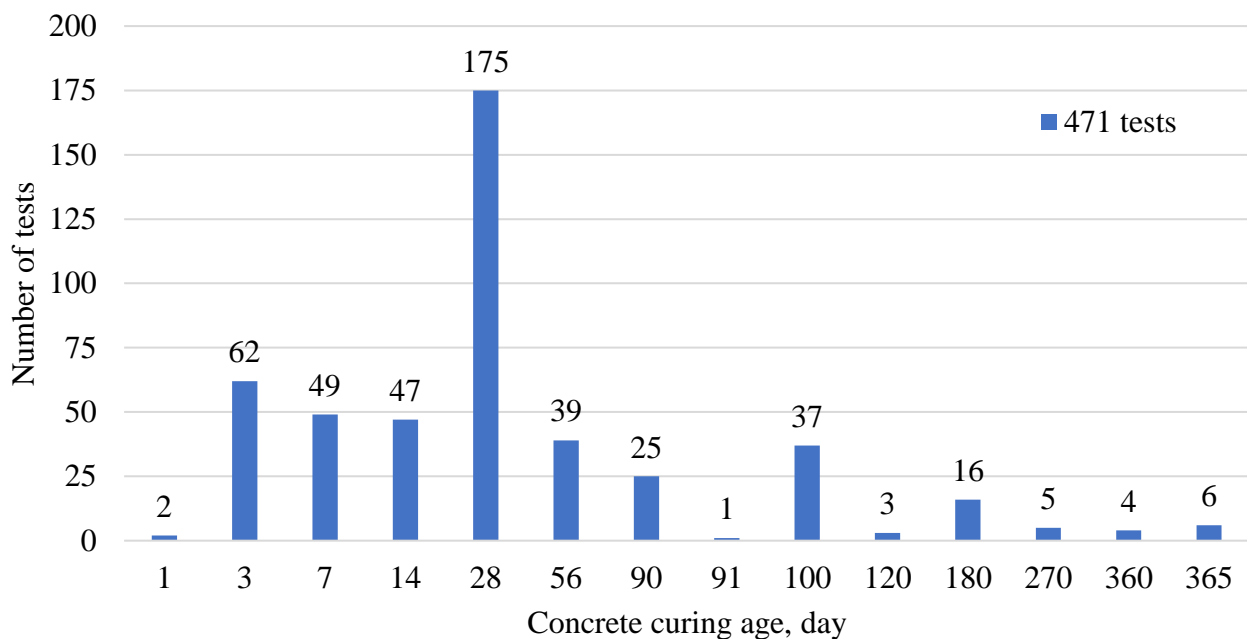
Figure 1 – Number of compression tests per concrete curing age [9]

The analysis was made in the following sequence:
1) Determining the number of compositions (including those containing fly ash) tested, by searching for rows with identical consumptions (in kg/m^3) of components (cement, fly ash, water, superplasticizer, coarse aggregate, fine aggregate).
2) Determining best compositions with fly ash in terms of compressive strength, by filtering tabular data per each testing age and defining the composition with the highest compressive strength value.
3) Determining the fraction of cement replacement with fly ash for the best compositions, by dividing its volume to the summed volume of cement and fly ash.
4) Analyzing the generalized effect of fly ash on the concrete compressive strength in different ages of curing, using graphical representation.
5) Defining the optimal composition with fly ash considering cumulative effect of fly ash consumption and compressive strength at the ages of 3 and 28 days, by weighted sum method [10].

3. Results and Discussion

Manipulation of the considered tabular data revealed that it presents results of compression tests of the 183 concrete compositions, including 95 containing fly ash. The compositions were tested at different curing ages, and those with fly ash were tested at the ages of 3, 14, 28, 56 and 100 days.

Table 1 below presents the list of best compositions of concrete utilizing fly ash that demonstrated highest compressive strength at one or several curing ages. Table also shows the fraction of fly ash in the binder combination.

Table 1 – Best compositions from [9]

Composition No.	Cement (kg/m^3)	Fly ash (kg/m^3)	Fraction of fly ash	Water (kg/m^3)	Superplasticizer (kg/m^3)	Coarse aggregate (kg/m^3)	Fine aggregate (kg/m^3)	Age* (day)	Concrete compressive strength (MPa)
1	246.83	125,08	33.6%	143.3	11.99	1086.8	800.89	3	23.52
								14	42.22
								28	52.5
								56	60.32
								100	66.42
2	275.07	121,35	30.6%	159.48	9.9	1053.6	777.5	3	23.8
								14	38.77
								28	51.33
								56	56.85
3	252.31	98,75	28.1%	146.25	14.17	987.76	889.01	3	21.78
								14	42.29
								28	50.6
								56	55.83
								100	60.95
4	505	60	11%	195	0	1030	630	28	64.02

* For some curing ages there was not tests performed

From the table above seen that there is no composition demonstrating the highest compressive strength all at once considered curing ages. However, plotting the highest compressive strength values for each curing age, regardless of composition, on a graph (Figure 2) provides valuable insights into the influence of fly ash on compressive strength at different stages of curing.

$r (\bullet, \blacklozenge) = -0,238$
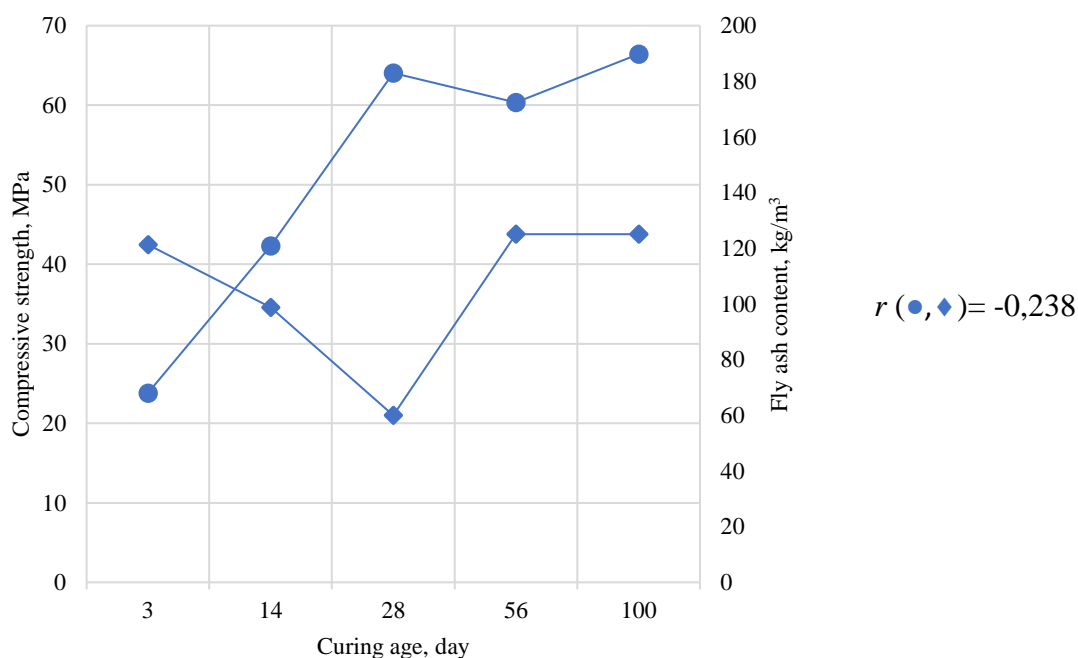
Figure 2 – Behavior of compressive strength vs. fly ash on different stages of concrete curing

The figure above shows the logical dynamics of compressive strength when the content of fly ash changes: the less the amount of fly ash the more the value of compressive strength. This denotes their inversely relationship, which is proven by the minor negative correlation factor *r* equal to -0,237 between these values. Despite this fact, there is still potential to select concrete compositions complying certain levels of compressive strength required saving a cement binder by replacing it partially by fly ash.

More thorough investigation of Table 1 above shows that it contains 3 or more values of concrete strength up to 56 days of curing, which helps to deduce certain patterns (Figure 3) for further analyzing the generalized effect of fly ash.

$$y = 9.528\ln(x) - 9.5884$$
$$R^2 = 0.6059$$

a)

$$y = 40.857x^{0.0015}$$
$$R^2 = 3E\text{-}06$$

b)

$$y = 101.46x^{-0.198}$$
$$R^2 = 0.9404$$

c)

$$y = 37.176e^{0.0143x}$$
$$R^2 = 0.9428$$

d)
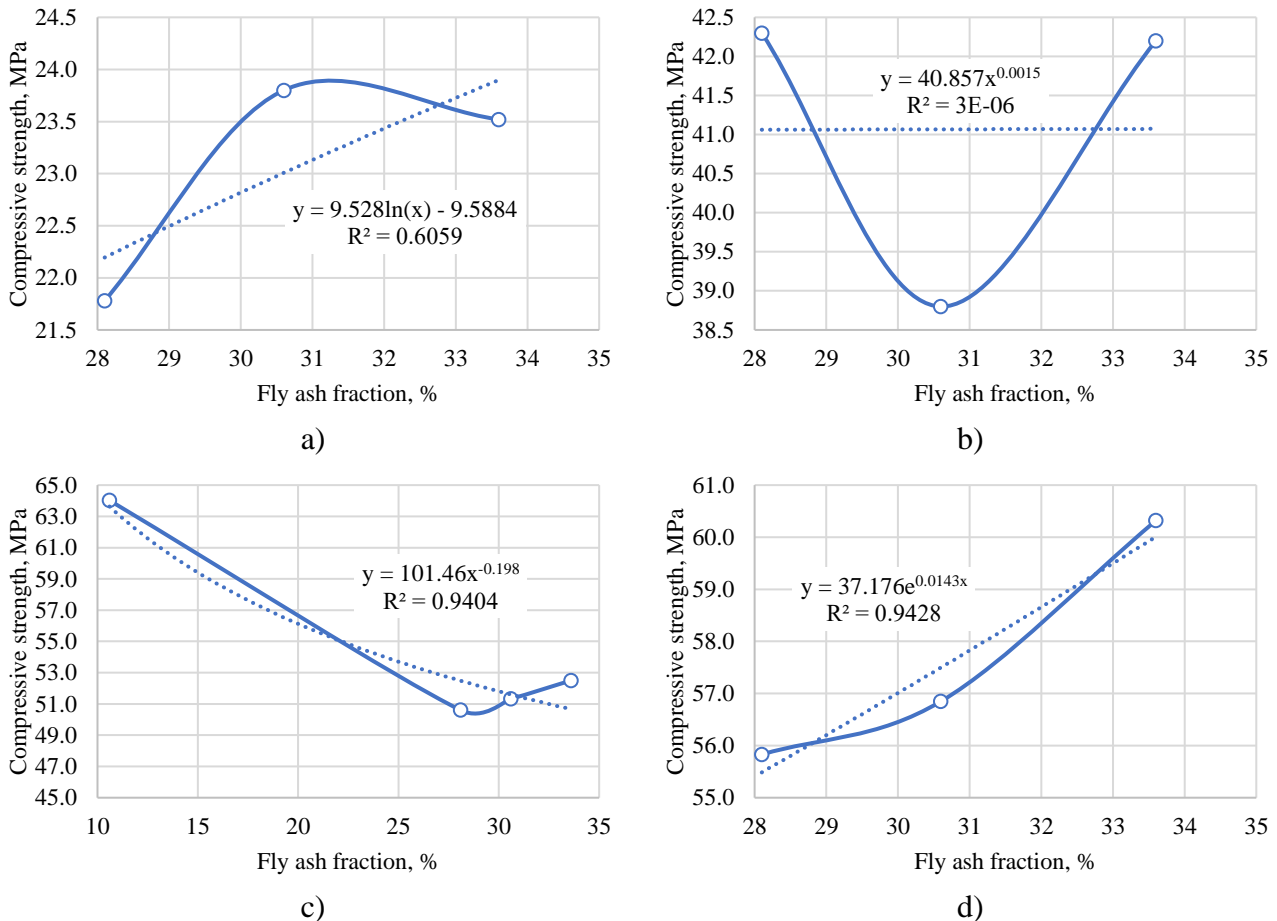
Figure 3 – Effect of fly ash on concrete strength for various curing ages: a) 3 days; b) 14 days; c) 28 days; d) 56 days.

From the figures above seen that increase in the fly ash fraction affects compressive strength variously, depending on the curing age. Thus, at the age of 3 days, an increase in the fly ash fraction to 31% led to the sharp increase in the compressive strength, but its further increase led to slight decrease of the compressive strength. The logarithmic function characterizing such pattern appeared best suiting. However, its coefficient of determination R^2 turned out to be a little weak, being equal to 0,6059, which makes that function inefficient for the considered period. At the age of 14 days, we can see even worse situation, where there is not much of a pattern. Further periods of concrete curing (28 and 56 days) showed notable patterns. Here, the increase in the fly ash fraction up to 28% had no positive effect on the compressive strength. But its further increase led to stable growth of the compressive strength.

The weighting (y) of the values of such parameters of concrete compositions as fly ash fraction and compressive strength at the curing ages of 3 and 28 days and summing them showed the following noteworthy result (Figure 4).

Composition No.	y_f	y_3	y_{28}	$y_f + y_3 + y_{28}$
1	0.327	0.255	0.240	0.822
2	0.297	0.258	0.235	0.791
3	0.273	0.236	0.232	0.741
4	0.103	0.250	0.293	0.646
$\sum y$	1	1	1	

Figure 4 – Weighted sum and ranking

As seen from the figure above, weight of the fraction of fly ash is arranged in descending order from the 1st to the 4th composition. However, it is not the case for the weights of the compressive strength at the age of 3 days, where the 2nd composition showed the highest weight. The highest weight of the compressive strength at the age of 28 days goes to the 4th composition. Cumulatively, the weighted sum suggests as the optimal composition No. 1.

4. Conclusions

1. The compressive strength of concrete exhibits an inverse relationship with the content of fly ash. A minor negative correlation factor ($r = -0.237$) validates the inverse relationship. Despite the inverse relationship, there remains the potential to optimize the concrete composition for specific compressive strength requirements by partially replacing cement binder with fly ash.

2. The influence of fly ash on compressive strength changes depending on the concrete's curing age. Initially, at 3 days, adding up to 30.6% fly ash enhances compressive strength, followed by a decrease with further increments. Although a logarithmic function captures this trend, its coefficient of determination ($R^2 = 0.6059$) is relatively weak. At 14 days, no clear trend is evident, but distinct patterns emerge at 28 and 56 days. Specifically, there's no enhancement in compressive strength with fly ash fractions up to 28.1%, but a consistent increase occurs with higher fractions.

3. The weighted sum analysis, cumulatively incorporating fly ash fraction and compressive strength at 3 and 28 days, designates composition with fly ash replacing 33.6% of cement binder as the optimal choice in the long term.

References

1. Fly Ash-Based Eco-Efficient Concretes: A Comprehensive Review of the Short-Term Properties / M. Amran, R. Fediuk, G. Murali, S. Avudaiappan, T. Ozbakkaloglu, N. Vatin, M. Karelina, S. Klyuev, A. Gholampour // Materials. — 2021. — Vol. 14, No. 15. — P. 4264. https://doi.org/10.3390/ma14154264
2. Characteristics and applications of fly ash as a sustainable construction material: A state-of-the-art review / G. Xu, X. Shi // Resources, Conservation and Recycling. — 2018. — Vol. 136. — P. 95–109. https://doi.org/10.1016/j.resconrec.2018.04.010
3. Effect of Fly Ash as Partial Cement Replacement on Workability and Compressive Strength of Palm Oil Clinker Lightweight Concrete / N. Ghazali, K. Muthusamy, R. Embong, I.S.A. Rahim, N.F. Muhamad Razali, F.M. Yahaya, N.F. Ariffin, S. Wan Ahmad // IOP Conference Series: Earth and Environmental Science. — 2021. — Vol. 682, No. 1. — P. 012038. https://doi.org/10.1088/1755-1315/682/1/012038
4. Fly ash for sustainable construction: A review of fly ash concrete and its beneficial use case studies / D.K. Nayak, P.P. Abhilash, R. Singh, R. Kumar, V. Kumar // Cleaner Materials. — 2022. — Vol. 6. — P. 100143. https://doi.org/10.1016/j.clema.2022.100143
5. Fly ash – waste management and overview : A Review / A. Dwivedi, M.K. Jain // Recent Research in Science and Technology. — 2014. — Vol. 6, No. 1. — P. 30–35.
6. Durability research of high performance concrete and its application in engineering / J. Wu // Applied and Computational Engineering. — 2023. — Vol. 25, No. 1. — P. 109–116. https://doi.org/10.54254/2755-2721/25/20230746
7. Advancements in low-carbon concrete as a construction material for the sustainable built environment / F. Althoey, W.S. Ansari, M. Sufian, A.F. Deifalla // Developments in the Built Environment. — 2023. — Vol. 16. — P. 100284. https://doi.org/10.1016/j.dibe.2023.100284
8. Cement and concrete as an engineering material: An historic appraisal and case study analysis / C.R. Gagg // Engineering Failure Analysis. — 2014. — Vol. 40. — P. 114–140. https://doi.org/10.1016/j.engfailanal.2014.02.004

9. Fly ash concrete / P. Van Ngoc // Mendeley Data. — 2023. — Vol. 1. https://doi.org/10.17632/C8G7SMDGZS.1
10. Multi-Objective Optimization / X.-S. Yang // Nature-Inspired Optimization AlgorithmsElsevier, 2014. — P. 197–211. https://doi.org/10.1016/B978-0-12-416743-8.00014-2

Information about authors:

Sungat Akhazhanov – PhD, Associate Professor, Department of Algebra, Mathematical Logic and Geometry named after T.G. Mustafin, Karaganda Buketov University, Karaganda, Kazakhstan, stjg@mail.ru

Gulshat Tleulenova – PhD, Acting Associate Professor, Department of Civil Engineering, L.N. Gumilyov Eurasian National University, Astana, Kazakhstan, gulshattleulenova23@mail.ru

Sabit Karaulov – Junior Researcher, Solid Research Group, LLP, Astana, Kazakhstan, karaulovsabit1997@gmail.com

Shyngys Zharassov – MSc, Junior Research Scientist, Research laboratory of applied mechanics and robotics, Karaganda Buketov University, Karaganda, Kazakhstan, zhshzh95@gmail.com

Alisher Mukhamejan – Bachelor Student, Department of Civil Engineering, L.N. Gumilyov Eurasian National University, Astana, Kazakhstan, alisher.2403@mail.ru

Author Contributions:

Sungat Akhazhanov – concept, funding acquisition, editing.
Gulshat Tleulenova – methodology, analysis.
Sabit Karaulov – visualization, modeling.
Shyngys Zharassov – resources, interpretation, drafting.
Alisher Mukhamejan – data collection, testing.

Article

Study of the pore structure of foam concrete using a two-stage foaming method

Rauan Lukpanov[1,2], Duman Dyussembinov[1], Zhibek Zhantlessova[1,2,*],

Aliya Altynbekova[1,2], Anatolij Smoljaninov[3]

[1]Solid Research Group, LLP, 010008, Tashenova str., 27, Astana, Kazakhstan
[2]Department of Technology of Industrial and Civil Construction, L.N. Gumilyov Eurasian National University, 010008, Satpayev str., 2, Astana, Kazakhstan
[3]ProfiOffice GmbH, Mergenbaum-Platz, 4, 63741, Aschaffenburg, Germany
*Correspondence: proyekt.2022@bk.ru

Abstract. This study presents an in-depth analysis of the pore structure in foam concrete, manufactured using a novel two-stage foam introduction method, with a comparative assessment against traditional foam concrete. Pore structure evaluation was conducted through visual-instrumental inspection and measurements of pore areas in segmented samples, including upper, middle, and lower segments. The results indicate that the proposed foam introduction method Type 1 results in a more stable pore structure distribution compared to classical foam concrete Type 2. In the upper segment, Type 1 samples exhibit an average pore content of 28.977%, while Type 2 samples show 36.112%. Similarly, in the middle segment, Type 1 samples display 27.147%, and Type 2 samples demonstrate 28.410%. The lower segment of Type 1 samples displays 24.054%, with Type 2 samples showing 22.136%. The differences in pore volumes between the lower and upper segments are 12% for Type 1 and 27.11% for Type 2, demonstrating a significant variation in the quality of the pore structure. This research sheds light on the advantages of the proposed two-stage foam introduction method in enhancing the stability and quality of foam concrete's pore structure, with potential implications for its use in various construction applications.
Keywords: foam, foam concrete, two-stage foaming, pore structure, injection.

1. Introduction

One of the primary driving forces behind the development of construction is the invention and implementation of new materials and production technologies, including innovations in concrete technology [1-3]. This article examines the modernization of the technological process for producing foam concrete, a type of lightweight concrete. Currently, a significant portion of lightweight concrete used in construction is composed of aerated concrete (or aerated concrete blocks), primarily due to the relative simplicity of its production compared to foam concrete.

When comparing foam concrete with aerated concrete, as offered in the market, the proposed foam concrete presents several logical advantages:

- It allows for the production of monolithic structures on the construction site, unlike aerated concrete. This is because aerated concrete expands during the hardening process, making it challenging to maintain precise geometric dimensions for construction elements, which are crucial for quality and reliability [4].

- Horizontal structures made of monolithic foam concrete can be easily produced, while doing so with aerated concrete is labor-intensive and not cost-effective. This is because aerated concrete blocks are assembly elements without reinforcement, and they are not designed to withstand significant lateral stresses [5].

- When comparing foam concrete and aerated concrete with equal strength, a structure, such as a wall, made of monolithic foam concrete was exhibit higher compressive and tensile strength than a structure made of assembled aerated blocks. In the case of compression, the distribution of stress and deformation in monolithic foam concrete is more uniform, unlike aerated blocks, and in the case of tension, the strength of aerated blocks is limited by the adhesive bond.

- The monolithic nature of foam concrete provides the construction with greater stability compared to assembled aerated blocks. It improves the resistance of the structure to bending in both the plane and out of the plane [6].

- The ability to perform spatial reinforcement of load-bearing foam concrete structures expands the range of applications for the material compared to assembled aerated blocks [7].

One drawback of foam concrete is the relatively complex assembly of structures, which requires additional formwork. However, with established serial production, this drawback is offset by the complexity of masonry work with aerated blocks and the need for longitudinal reinforcement of the assembly, which is not provided in the aerated block structure (i.e., manual groove cutting is required in aerated blocks) [8].

Undoubtedly, foam concrete has certain advantages over aerated concrete, such as a closed pore structure, which makes it stronger due to a more robust skeleton structure. It also offers relative durability, given the presence of cementitious binding components, as opposed to aerated concrete that includes lime-gypsum binding, which is less resistant to mechanical stress, especially exposure to water. However, these advantages remain theoretical since, under otherwise identical conditions (material reliability and durability), the simplification of the production process becomes the prevailing advantage.

This article was present research on the durability of the proposed foam concrete production method compared to the classical method [9].

2. Methods

The proposed method for producing foam concrete, as opposed to the classical method, involves a two-stage introduction of foam. The initial introduction of a low-concentration foam solution takes place during the preparation of the sand-cement mixture, thereby improving its workability and reducing the water-cement ratio (thus minimizing foam quenching by water) [10]. Subsequently, during the secondary introduction of a high-concentration foam solution in the foam concrete structure manufacturing stage, the reduction in the water-cement ratio allows for maximum preservation of the initial foam concentrate multiplicity and contributes to the formation of a uniform porous material structure. Figure 1 presents a schematic representation of the foam concrete production process using the proposed method.
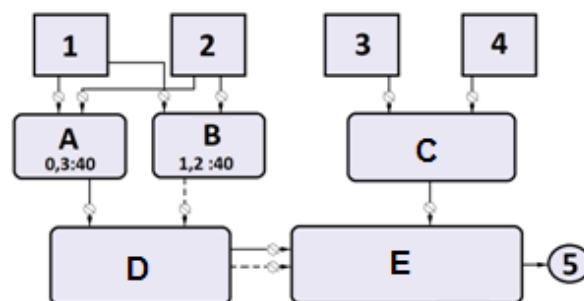
A - container for low-concentrated solution of plasticising foam concentrate additive in water 0,23:85 l; B - container for solution of modified foam concentrate in water 1,2:40 l; C - cement-sand mixer; D - foam generator; E - mortar mixer; ⊘ - dosing unit; ——➤ - primary foam injection; --➤ - secondary foam injection.

Figure 1 – Foam concrete production scheme

To assess the pore structure of foam concrete, research involving direct and indirect tests was conducted. Direct evaluation of the pore structure included a visual examination of pores on the sample surface (Figure 2), both before and after strength testing. Inspection of samples before failure was carried out by tapping opposite faces of cubic-shaped samples, and after failure, by examining the internal fracture surfaces [11]. The comparative criterion used was an indicator characterizing the ratio of the pore area to the area of the inspected section (hereafter referred to as the porosity coefficient). Indirect methods for assessing pore distribution included tests of strength and density [12]. The difference in sample densities provided a quantitative assessment of the material's pore structure. Since the composition of the samples was identical for both methods, lower density would indicate a greater number of pores in the sample. The difference in strengths, in turn, indirectly characterized the quality of the pore structure of the samples, where the result could be influenced not only by the size of the pores but also by their uniform distribution and the presence of micropores in the skeleton walls [13].

To determine the porosity coefficient, the following operations were performed:

- photographs of sections of foam concrete samples were taken, using pre-marked areas.

- the photographs were converted into a graphic editor for digital counting of the total pore area within the marked sections.

Immediately before inspecting the samples (blocks), the areas to be examined were marked (9 sections) in terms of both height and width of the sample (3 sections of 5x5 cm at each height). The height gradation was associated with an assessment of potential non-uniform pore distribution along the sample's height due to more substantial foam quenching at the lower part. AutoCAD was used as the graphic editor. To calculate the pore area, the inspected area was first scaled to match real dimensions. Then, all pore contours on the section were traced using isolines, followed by automated area calculations.
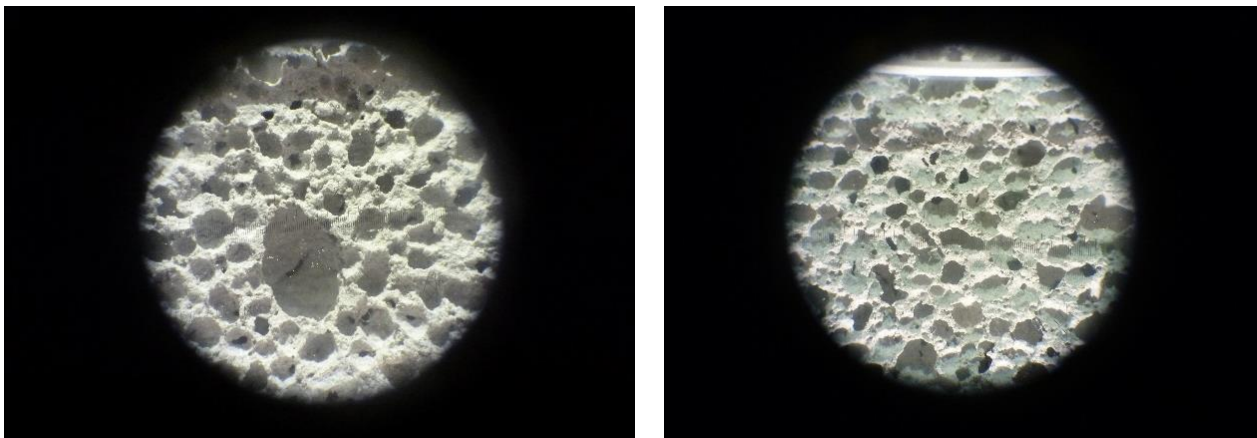
Figure 2 – Pore structure of foam concrete samples

To determine the density and strength of foam concrete blocks, they were segmented into lower, middle, and upper parts by height (Figure 2). From each segment, square-shaped samples (10x10 cm) were selected. The reason for segmenting the samples vertically was also related to the potential non-uniform distribution of pores along the height.

The technological composition of the compared types of foam concrete samples is presented in Table 1.

Table 1 – Technological composition of compared sample types

Type	Cement M400, kg	Fine sand, kg	Ratio of blowing agent to water at primary injection, g:l	Ratio of blowing agent to water at secondary injection, g:l	Water, l	Foam concentrate, g
Type 1	350	250	0.23:85	1.27:40	-	-
Type 2	350	250	-	-	175	1.5

3. Results and Discussion

Figures 3-5 present the results of the quantitative assessment of the pore structure through visual-instrumental inspection of the samples. Figure 3 shows the results of inspections for the upper segments of foam concrete blocks, Figure 4 presents the same inspections for the middle segments, and Figure 5 displays the results for the lower segments. The specific values (data points) of the percentage of pore area to the inspection area were sorted in ascending order for a better understanding of patterns (to visually highlight the differences between the compared types of foam concrete). In other words, the depicted curves do not represent any particular pattern but only indicate differences in pore dimensions.
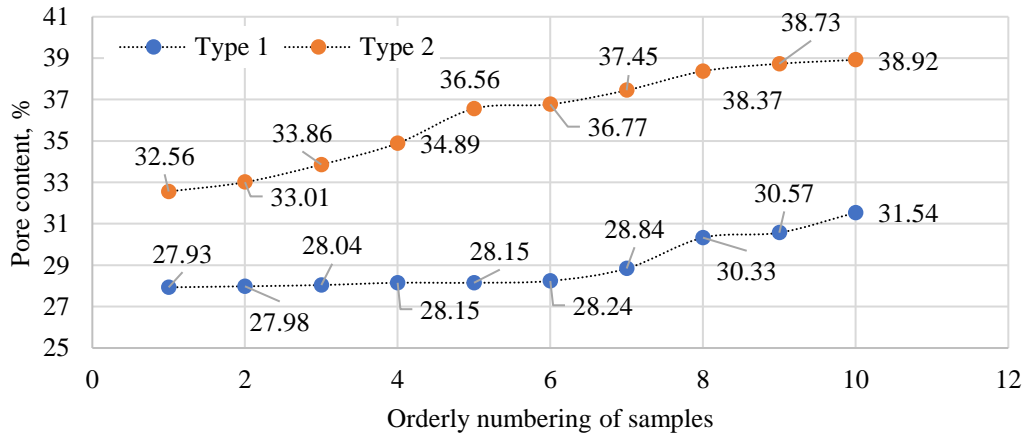
Figure 3 – Evaluation of the upper segments of the samples
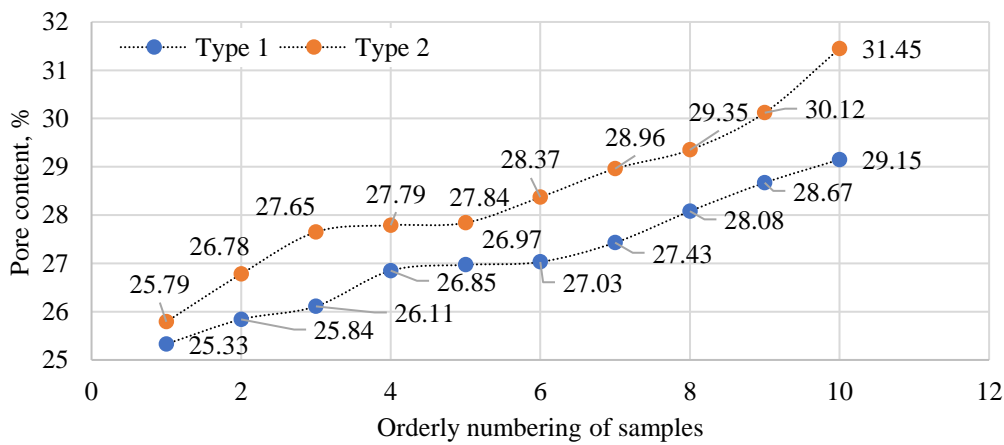
Figure 4 – Estimation of average sample segments
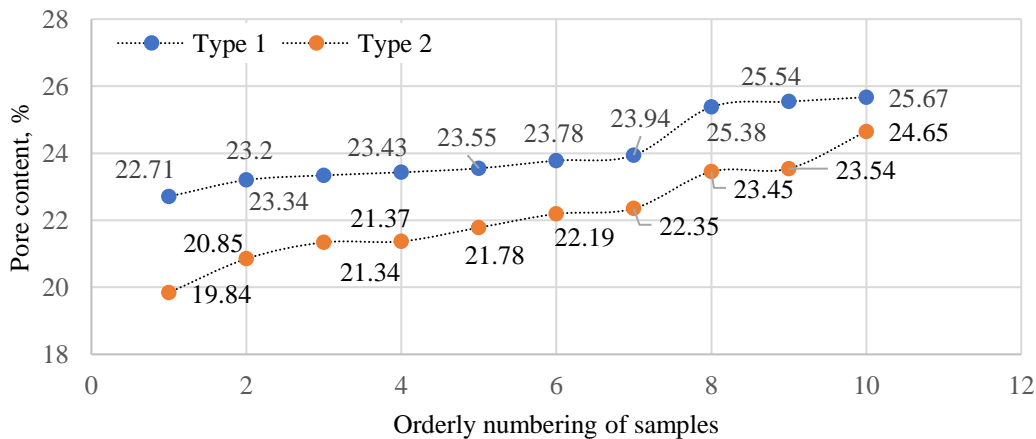
Figure 5 – Assessment of lower segments of samples

According to the results, the percentage distribution of pore content in the upper segments of type 1 samples falls within the range of 27.93% to 31.54%, which is relatively lower than the distribution of type 2 samples, ranging from 32.56% to 38.92%. In the middle segments, a similar pattern is observed in terms of percentage pore content, but the results are quantitatively very close: for type 1 samples, the range is within 25.33% to 29.15%, and for type 2 samples, it is 25.79% to 31.45%. Opposite results are observed in the lower segments. For type 1 samples, the percentage distribution of pore content exceeds that of type 2 samples: for type 1, the range is 22.71% to 25.67%, while for type 2, it is 19.84% to 24.65%.

Figure 6 illustrates the difference in pore distributions across the sample segments (upper, middle, and lower). According to the diagrams, the difference in pore sizes between type 1 and type 2 in the upper segments ranges from 10% to 39%, in the middle segments from 1% to 16%, and in the lower segments from -1% to -17%. Negative values indicate that the density of the lower segments is significantly lower than that of the upper segments, considering the overall trend in density distribution vertically in the foam concrete samples. All obtained data points have a relatively strong correlation and can be considered reliable. Statistical data are presented in Table 2.
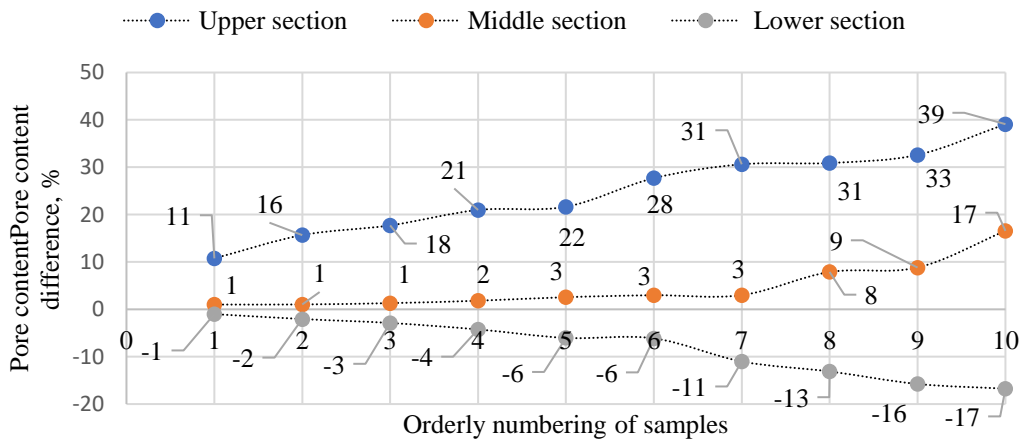
Figure 6 - Percentage difference of pore distribution

Table 2 – Statistical data points

Indicator	Upper section		Middle section		Lower section	
	Type 1	Type 2	Type 1	Type 2	Type 1	Type 2
Mean value, %	28.977	36.112	27.146	28.410	24.054	22.136
Quadratic deviation	1.326	2.382	1.225	1.638	1.073	1.427
Coefficient of variation	4.578	6.596	4.512	5.767	4.459	6.449

The average pore content for all type 1 samples in the upper segment is 28.977%, while for type 2 samples, it is 36.112%. The average pore content in the middle segment of type 1 samples is 27.147%, and for type 2 samples, it is 28.410%. In the lower segment of type 1 samples, the average pore content is 24.054%, and for type 2 samples, it is 22.136%. It should be noted that all data points within the segments (upper, middle, and lower) do not exhibit significant deviations from the mean, with coefficients of variation in all cases not exceeding 7%. However, it is important to note that for type 2 samples, the coefficients of variation on all segments exceed those of type 1 by 27-44%. This suggests that the pore structure of type 2 samples is less stable than that of type 1, as the data points for type 1 samples deviate more from each other, indicating a lower confidence level. According to the obtained data, a general pattern of pore distribution along the sample height is observed, as

evidenced by the diagram in Figure 7, which displays the average pore distribution values along the vertical axis. The segments are conditionally labeled on the y-axis (ordinate axis): 1 – lower segment, 2 – middle segment, 3 – upper segment.
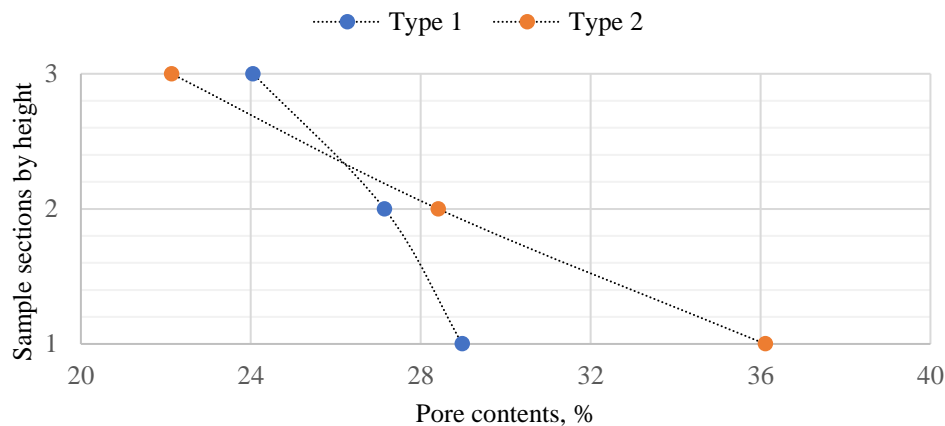
Figure 7 – Pore structure distribution by height

According to the provided diagram, non-uniformity in the distribution of the pore structure along the vertical axis is observed. Comparing the average values for the segments, for type 2 samples, the percentage pore content is (from bottom to top): 24.05%, 27.15%, 28.98%. The difference between the lower and upper segments in type 1 samples is 12%, and between the middle and upper segments is 6%. The same parameters for type 2 samples are (from bottom to top): 22.14%, 28.41%, 36.11%. However, the difference between the segments significantly exceeds (compared to type 1), amounting to 27.11% and 28.34%, respectively. This indicates the quality of the pore structure in the samples: type 2 samples show a substantial increase in pore volume along the sample height, whereas in type 1 samples, the increase in pore content along the height is significantly lower. This pattern is also evident in the slope of the curves, with a steeper slope indicating greater deviations from the mean value. Numerically, the maximum deviations for type 1 samples are 8.4% and 11.11% (for the upper and lower segments), while for type 2 samples, the same figures are 25.02% and 30.49%, respectively.

4. Conclusions

1. A comprehensive study of cellular concrete samples (foam concrete produced by the proposed two-stage method, classical foam concrete, and autoclaved aerated concrete) was conducted to assess their pore structure. The evaluation of pore distribution was carried out through visual-instrumental inspection and measurements of pore areas in segmented samples (divided into three vertical segments: upper, middle, and lower). The assessment was performed in comparison with classical foam concrete.

2. According to the results, the pore structure distribution is more stable in samples manufactured by the proposed method (Type 1) compared to samples of classical foam concrete (Type 2). This is evidenced by the obtained data points of percentage pore content: the average pore content for all Type 1 samples in the upper segment is 28.977%, while for Type 2 samples, it is 36.112%; in the middle segment of Type 1 samples, it is 27.147%, and for Type 2 samples, it is 28.410%; in the lower segment of Type 1 samples, it is 24.054%, and for Type 2 samples, it is 22.136%.

3. The difference in pore volumes in Type 1 samples between the lower and upper segments is 12%, and between the middle and upper segments, it is 6%. The same parameters for Type 2 samples are (from bottom to top): 22.14%, 28.41%, 36.11%. However, the difference between the

segments significantly exceeds that of Type 1, amounting to 27.11% and 28.34%, respectively. This indicates the quality of the pore structure in the samples: Type 2 samples exhibit a substantial increase in pore volumes along the sample height, while in Type 1 samples, the increase in pore content along the height is significantly lower.

Acknowledgments

References

1. Research of foam concrete components in the regional production conditions of Nur-Sultan / R. Lukpanov, D. Dyussembinov, A. Altynbekova, Z. Zhantlesova // Technobius. — 2022. — Vol. 2, No. 3. — P. 0023. https://doi.org/10.54355/tbus/2.3.2022.0023
2. Approximative approach to optimize concrete foaming concentration in two stage foaming / R. Lukpanov, D. Dyussembinov, A. Altynbekova, Z. Zhantlesova // Technobius. — 2023, Vol. 3, No. 3. — P. 0041. https://doi.org/10.54355/tbus/3.3.2023.0041
3. Research on the Effect of Post-alcohol Bard on the Properties of the Cement-Sand Mixture. / Lukpanov, R.E., Dyussembinov, D.S., Altynbekova, A.D., Yenkebayev, S.B. // Industrial and Civil Construction 2022 ISCICC 2022. Lecture Notes in Civil Engineering. — 2024. — Vol. 436. — P. 107-113. https://doi.org/10.1007/978-3-031-44432-6_14
4. A classification of studies on properties of foam concrete / K. Ramamurthy, E.K.K. Nambiar, G.I.S. Ranjani // Cement & Concrete Composites. — 2009. — Vol. 31, No. 6. — P. 388-396. https://doi.org/10.1016/j.cemconcomp.2009.04.006
5. Experimental investigation on cement-based foam developed to prevent spontaneous combustion of coal by plugging air leakage / X. Xi, S. Jiang, C. Yin, Z. Wu // Fuel. — 2021. — Vol. 301. — P. 121091. https://doi.org/10.1016/j.fuel.2021.121091
6. Chemical Blowing Agent Systems for Polymer Foam Manufacture / O'Connor Christopher. — Oxford, UK: The University of Manchester, 1999.
7. Development of macro/nanocellular foams in polymer nanocomposites / Bhattacharya Subhendu. — RMIT University, 2009.
8. Chemical admixtures — Chemistry, applications and their impact on concrete microstructure and durability / J. Plank, E. Sakai, C.W. Miao, C. Yu, J.X. Hong // Cement and Concrete Research. — 2015. — Vol. 78, No. 1. — P. 81–99. https://doi.org/10.1016/j.cemconres.2015.05.016
9. GOST 31108-2016 General Construction Cements. — 2016.
10. GOST 310.3-76 Cements. Methods for determining the normal density, setting time and volume change uniformity. — 1976.
11. GOST 8736-2014 Sand for construction works. — 2014.
12. TU 5870-002-14153664-04 Complex additives for concrete and mortars. — 2005.
13. GOST 12730.1-2020 Concretes. Methods of determination of density. — 2020.

Information about authors:
Rauan Lukpanov – PhD, Professor, Scientific Supervisor, Solid Research Group, LLP, 010008, Tashenova str., 27, Astana, Kazakhstan, rauan_82@mail.ru
Duman Dyussembinov – Candidate of Technical Sciences, Associate Professor, Senior Researcher, Solid Research Group, LLP, 010008, Tashenova str., 27, Astana, Kazakhstan, dusembinov@mail.ru
Zhibek Zhantlesova – Junior Researcher, Solid Research Group, LLP, 010008, Tashenova str., 27, Astana, Kazakhstan; PhD Student, Department of Technology of Industrial and Civil Construction, L.N. Gumilyov Eurasian National University, 010008, Satpayev str., 2, Astana, Kazakhstan, zhibek81@mail.ru
Aliya Altynbekova – Researcher, Solid Research Group, LLP, 010008, Tashenova str., 27, Astana, Kazakhstan; PhD Student, Senior Lecturer, Department of Technology of Industrial and Civil Construction, L.N. Gumilyov Eurasian National University, 010008, Satpayev str., 2, Astana, Kazakhstan, kleo-14@mail.ru

Anatolij Smoljaninov – Candidate of Physical and Mathematical Sciences, Expert, ProfiOffice GmbH, Mergenbaum-Platz, 4, 63741, Aschaffenburg, Germany, <u>nts.kazakstan@gmail.com</u>

Author Contributions:
Rauan Lukpanov – concept, methodology, funding acquisition.
Duman Dyussembinov – resources, modeling, analysis.
Aliya Altynbekova – data collection, testing.
Zhibek Zhantlesova – visualization, drafting.
Anatolij Smoljaninov – interpretation, editing.

Technobius

https://technobius.kz/

Article

Ways to address the construction of new buildings in old urban areas

Aliya Aldungarova[1,2], Assel Mukhamejanova[1,3*], Nurgul Alibekova[3], Aleksej Aniskin[4]

[1]Solid Research Group, LLP, Astana, Kazakhstan
[2]School of Architecture, Civil Engineering and Energy, D. Serikbayev East Kazakhstan technical university, Ust-Kamenogorsk, Kazakhstan
[3]Department of Civil Engineering, L.N. Gumilyov Eurasian National University, Astana, Kazakhstan
[4]Department of Civil Engineering, University North, Varaždin, Croatia
*Correspondence: assel.84@list.ru

Abstract. This paper deals with the problem of constructing new buildings in old urban areas, with emphasis on determining the actual dimensions of the active footprint of existing foundations. The study focuses on the problems associated with limited space for construction, geotechnical conditions, soil characteristics, as well as the features of near-surface foundations and methods for calculating their settlement. The paper proposes a methodology that, when applied, provides a more accurate and reliable determination of non-uniformity of base deformations of neighboring foundations. This is achieved by taking into account a number of factors, such as the sequence of erection, soil compaction, the size of the footings and the magnitude of loads. The proposed approach also substantiates the optimal spacing of the designed neighboring foundations, helping to reduce the negative impact on existing structures and ensuring the stability and durability of both new and existing structures. The results of this study represent a significant contribution to the development of effective construction solutions in limited urban spaces, and can be used by designers and builders to optimize construction processes and ensure the stability of buildings in complex geotechnical conditions.

Keywords: old urban areas, near-surface foundations, settlement calculations, geotechnical conditions, building design.

1. Introduction

In the design of new buildings in older urban areas where construction by superstructure or additions to existing buildings is envisioned, there is a need to determine the actual footprint of the existing foundation footprint [1]. This active zone includes changes in the compressibility characteristics of soils subjected to long-term compaction and local changes in the stress-strain state of the foundation due to the additional load on the area [2]. Foundations for new buildings in old urban or built-up areas are very demanding and are usually conditioned to eliminate impacts to the surrounding development. The presence of a vacant lot in an old urban area indicates the presence of unfavorable geotechnical conditions or any other problems on the site [3]. The presence of surrounding buildings and limited space for organizing the construction site represent the main problems in the design and construction of a new building. In recent years, intensive construction has started on one of the vacant areas near the center of the old town [4].

Traditional methods of settlement calculation, including those regulated by standards and based on the theory of linearly deformed bodies, cannot accurately predict the actual size of the active (compacted) zone of the foundation. These methods are designed to calculate a conventional, idealized soil, which leads to overestimated values of the results, the deviation of which may exceed 100%. In this regard, such methods are not acceptable for calculating settlement of foundations of

buildings that are reconstructed in an urban environment, taking into account local changes in soil properties [5].

Therefore, for successful construction of buildings and structures in built-up areas, the results of studies of the behavior of closely spaced foundations are of particular importance. Special attention is paid to the formation of stress-strain zones and changes in physical and mechanical properties of soils subjected to long-term compaction during operation.

The purpose of the study is to analyze the influence of the stress zones of the new foundation on the formation of additional settlement of the existing foundation, taking into account the significant slope of the existing foundation under unilateral loading, and to determine the maximum allowable foundation spacing in accordance with the regulatory requirements.

2. Methods

The pattern of development of unequal settlement of adjacent foundations due to their mutual influence depends on several factors, such as the compressibility of soils, the sequence of load application and its magnitude, and the distance between adjacent foundations [6].

Unilateral impact on the foundation can lead to negative consequences such as tilt, roll, uneven settlement of foundations, distortion and misalignment of building structures [7]. Therefore, it is necessary to take this fact into account when designing, especially when calculating the deformation of the bases of closely located structures.

Let us assume that a new foundation F-2 is built next to an existing foundation F-1, under which the soil is partially compacted within the active zone 1 of the foundation (Figure 1). As a result, both foundations will undergo additional settlement, which will cause both foundations to tilt towards the newly constructed foundation. Taking these interactions into account is very important when analyzing the settlement development of their foundations in this case.
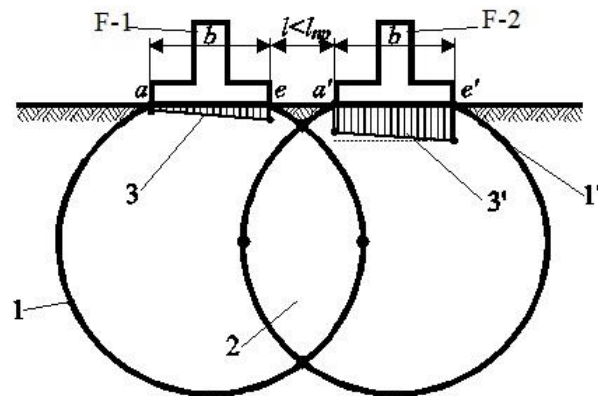
Figure 1 - Calculation diagram of the base of closely built foundations: 1 and 1' – boundaries of the active zones of the foundations F-1 and F-2; 2 – areas of overlap of active zones of bases; 3 – Estimated foundation settlement diagrams for foundations F-1 and F-2

In close proximity to the future structure is a residential building on Seyfullina Street in Astana, which is a five-story multi-family large-panel building, built around 1967 according to the project K-7 of the Mosproject Institute and belonging to the "Leningrad" series. The main load-bearing elements of this building are thin-walled reinforced concrete panels with thickened side ribs along the contour. The foundations of the house include columns of the cup type and reinforced concrete columns with cantilevers designed to support the basement panels. Basement waterlogging occurs due to the failure of the footings around the building and disturbance of the surrounding area. The strength of the concrete used in the structure is rated as B-25.

The construction site from a geological point of view is located on loam, which has light brown and brown colors. The soil has a different consistency, ranging from hard to soft-plastic. There are carbonate inclusions, as well as interlayers of sand and sandy loam up to 20 cm thick. The content of organic matter in the soil is up to 4.15%. The engineering-geological section at a depth of 15 meters is shown in Figure 2. The results of determinations of physical and mechanical properties of soils by engineering-geological elements are presented in Table 1.

Geological index	EGE	Subgrade depth, m	Layer thickness, m	Absolute mark, m	Description of soils	Well section	Depth, m	Groundwater Abs. elevation. Date of measurement
pdIV		0,40	0,40	348,35	Topsoil			
aQ/III-IV	1	3,40	3,00	345,35	Loam, light-brown and brown in color, from hard to soft-plastic consistency, with carbonate inclusions, with interlayers of sand and loam up to 20 cm thick, with admixture of organic matter up to 4.15%.		1 2 3	
	2	6,40	3,00	342,35	Loam, light brown and brown in color, of plastic consistency, with admixture of organic matter up to 3.88%, with interlayers of sand and loam up to 20 cm thick, of fluid consistency from a depth of 5.80 m.		4 5 6	▼344,65 01.12.21
	3	6,80	0,40	341,95	Sand of medium coarseness, brown color, water-saturated, polymictic composition.		7	
	4	8,10	1,30	340,65	The sand is coarse, brown and dark brown in color, water-saturated, polymictic composition, with interlayers of sand of different coarseness up to 20 cm thick.		8 9	
	5	11,50	3,40	337,25	Gravelly sand, brown and dark brown in color, water-saturated, polymictic composition, sand of different coarseness up to 20 cm thick.		10 11	
eC/I	6	12,40	0,90	336,35	Clay, burgundy-colored, of hard consistency, with inclusions of tarmac, in some places yellow-white, with spots of gelation and omarganization, with clay interlayers up to 20 cm thick.		12 13	
	7	15,00	2,60	333,75	Burgundy-colored loam, hard consistency, with inclusions of dresva, in some places yellow-white color, with spots of yellowing and omarganization, with clay interlayers up to 20 cm thick.		14 15	

Figure 2 – Engineering-geological section

Table 1 – Results of determinations of physical and mechanical properties of soils by engineering-geological elements

№ of EGE	Name of soil	Natural humidity, W, %	Density natural, ρ g/cm³	Density soil particle density, ρ_S g/cm³	Porosity coefficient, e	Compression module at natural humidity, E_{κ}, MPa	Angle of internal friction, φ, град.	Specific adhesion, C, MPa
№ 1 *aQ/III-IV)*	Loam, light brown to brown in color, hard to soft-plastic consistency	14.39	2.14	2.71	0.449	9.5	29.1	73
№ 2 *(aQ/III-IV)*	Loam, light brown to brown in color, solid to pourable consistency	23.28	2.04	2.70	0.636	5.5	12.8	38
№ 3 *(aQ/III-IV)*	Medium coarse sand, brown to dark brown in color, water saturated	14.83	1.56	2.3	0.650	30	35	1
№ 4 *(aQ/III-IV)*	Sand is coarse, brown and dark brown in color, water saturated	12.09	1.4	1.68	0.550	40	40	-
№ 5 *(aQ/III-IV)*	Gravelly sand, brown and dark brown in color, water saturated	9.79	1.46	1.75	0.650	30	38	-
№ 6 *(eC/I)*	Clay, burgundy in color, hard consistency	15.77	1.93	2.74	0.646	3.9	21.7	0.059
№ 7 *(eC/I)*	Loam, burgundy color, hard consistency	13.28	2.12	2.72	0.455	10.9	33.5	55

When planning new construction next to an existing building, both the maximum allowable additional deformations and the maximum allowable total deformations must be taken into account. Consequently, construction without preliminary determination of deformations in the existing building before the start of construction works, even if the recommendations on additional deformations are observed, does not guarantee protection against possible damage to the existing building. In this regard, it is planned to conduct a number of experimental studies to determine the allowable additional deformations, as well as to perform calculations using the finite element method.

Specialized dies were used to test adjacent dies. These rigid round disks with a flat sole or helical shape had sole areas ranging from 600 to 800 square centimeters. As part of the study, each die was loaded using a specialized design so that the pressure ranged from 0.01 to 0.1 MPa. The load at each level was kept centered and constant, and the total number of levels did not exceed 4. The duration of exposure at each level was the same, taking into account the conditional stabilization of ground rock deformation, which should not exceed 0.1 mm over a specified period of time according to state standard [8].

According to the state standard [9], the accuracy of settlement measurements when using deflection gauges was 0.1 mm. However, in some cases, more sensitive instruments such as IS and IP watch indicators were required, especially when studying compacted foundations of old built-up areas. The accuracy of measurements using these devices reached 0.01 mm.

Experiments conducted at both sites confirmed the relevance of the accepted working hypothesis of sequential effects on neighboring foundations. In the course of the experiments it became obvious that before the neighboring dies 2 (modeling new foundations) were subjected to loading, dies 1 (modeling old foundations) showed almost uniform settlement. The mutual influence of neighboring dies became more pronounced at the maximum load on die 2, which is due to a more complete overlap of the stress zones of the bases of both dies. Thus, the regularities of mutual influence of neighboring foundations established in the course of the experiment provide a basis for making appropriate corrections in the further improvement of soil investigation methods, as well as in the calculation and design of the geotechnical component of reconstructed buildings and structures.

The geotechnical model was analyzed by the finite element method using soil characteristics obtained from geotechnical investigations. When performing numerical studies on the settlement development of a foundation to be constructed in a built-up urban area, taking into account the compacted soils at the base, the calculation scheme presented in Figure 3 was used. The designed foundation F-2 is placed on the inhomogeneous, partially compacted base of the existing foundation F-1.
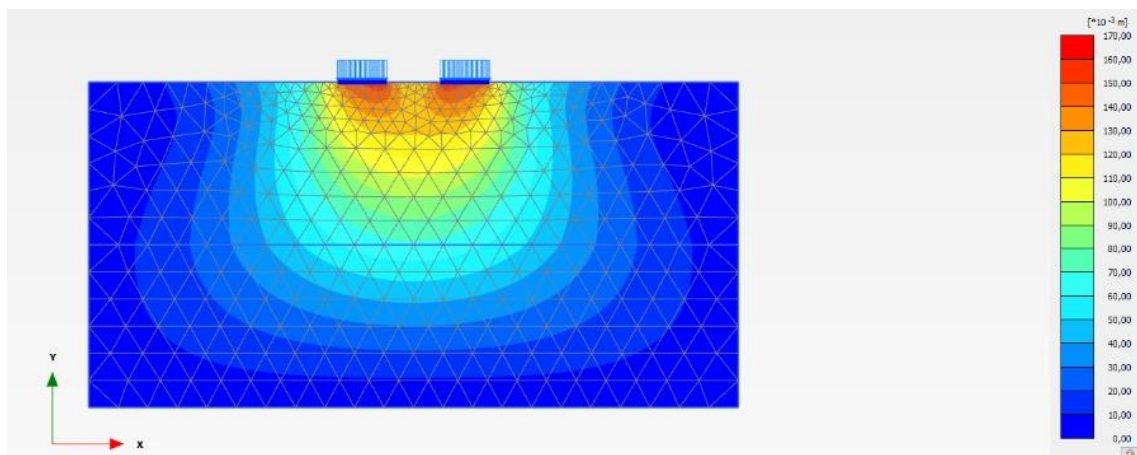
Figure 3 – Calculation scheme of neighboring foundations

3. Results and Discussion

Based on the results of both theoretical and experimental studies, we present a calculation model that assumes a pre-compaction of the soil to a state similar to the current state of the soil around the existing building. This model is based on the concept of volumetric compression of soils under the influence of maximum principal normal stresses, forming the actual deformed zone of the foundation footing. The use of a computer program is recommended for determining the volumes of complex-shaped overlay zones.

The new foundation F-2 is built next to the existing foundation F-1, under which the soil has already been compacted within the active zone 1 of the foundation, resulting in a significant reduction of its compressibility (Figure 4). In this case, the stresses caused by the loading of the new foundation F-2 in the overlap area 2 lead to additional compression of the already compacted foundation soil of the existing foundation F-1, which causes it to tilt towards the foundation to be erected. Thus, F-2 finds itself on a heterogeneous foundation, where on one side the soil is already compacted and on the other side it is in a natural state. It is obvious that, all other things being equal, the settlement of F-2, compared to an isolated foundation S built on naturally compacted soil, will be subject to change.

Settlement of the F-2 foundation built on inhomogeneous partially compacted basement will be less than:

$$S_{er.comp}^{imp} < S , \qquad (1)$$

hence we can take:

$$S_{er.comp}^{imp} = S - S_{dec.comp}^{imp}, \tag{2}$$

where $S_{er.comp}^{imp}$ - settlement of the foundation being constructed, influenced by the neighboring existing foundation;

$S_{dec.comp}^{imp}$ - reduction of settlement of the foundation influenced by the neighboring existing foundation, the value of which is determined from the following condition:

$$S_{dec.comp}^{imp} = S_{add.comp}^{imp}, \tag{3}$$

where $S_{add.comp}^{imp}$ - additional settlement of the existing foundation resulting from full loading of the neighboring foundation under construction.

Consequently, uneven settlements (rolls) of the neighboring foundations occurring under stepwise loading are caused by preliminary soil compaction in the area of overlap (overlap) of the active zones of the base of both foundations.

For the design of neighboring foundations, the settlement values are $S_{add.comp}^{imp} = S_{dec.comp}^{imp}$ it is recommended to determine the volumetric settlement method using a compression curve reflecting the law of compression of previously compacted soil, taking into account the overlapping stress zones of the bases of the interacting foundations..

The calculation of the additional settlement $S_{add.comp}^{imp}$ of the existing foundation should be determined by the formula:

$$S_{add.comp}^{imp} = S_{add.compI}^{imp}, S_{add.compII}^{imp}, S_{add.compIII}^{imp}, \tag{4}$$

where $S_{add.compI}^{imp}, S_{add.compII}^{imp}, S_{add.compIII}^{imp}$ - components of additional settlement of the existing foundation (F-1) due to subsequent compression of compacted zones (I, II and III) of its foundation under the influence of unequally stressed zones ((I, II and III) appearing in the foundation of the neighboring foundation under construction (F-2) at full loading.

Further, the settlement *S* of the designed foundation (F-2) should be determined without taking into account the factor of mutual influence, as for a foundation made of natural structure soil, and the following settlement values should be accepted (Figure 4): $S_a \leftrightharpoons S_e \leftrightharpoons S$.

The elements of the additional settlement presented according to the calculation scheme shown in Figure 4 form a settlement matrix. This matrix takes into account the overlapping stress zones of the foundations and therefore reflects the mutual influence of neighboring foundations on their settlement. Using the results of the existing foundation calculation (F-1), evaluate the adverse effect of the effect of partial compaction of the foundation on the settlement of the newly constructed foundation (F-2).

The calculation of the relative unevenness of settlement is checked from the following condition

$$\frac{S_{e'} - S_{a'}}{b} = \frac{S_{dec.comp}^{imp}}{b} \leq i_{marg}, \tag{5}$$

where $S_{e'} = S; S_{a'} = S - S_{dec.comp}^{imp}$.

And the distance between the designed foundations l should be checked based on the condition:

$$l \geq l_{marg}, \tag{6}$$

where l_{marg} – the maximum permissible distance between neighboring foundations at which the requirements of the normative document are met [10].
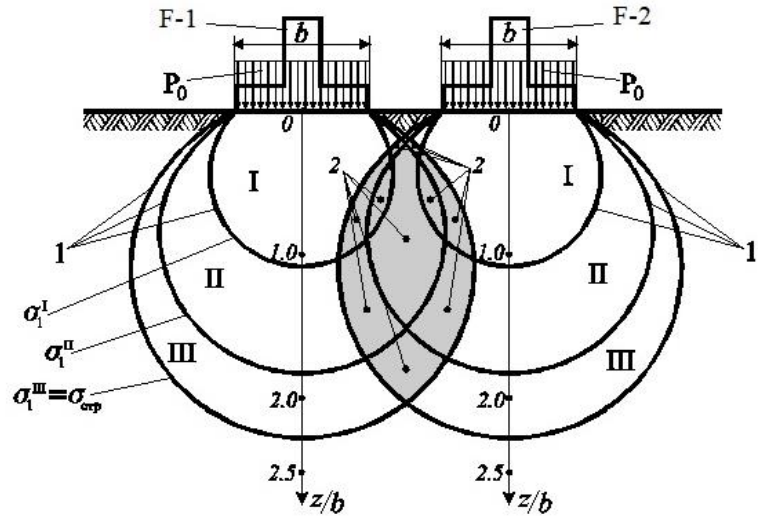
Figure 4 - Calculation scheme of the base of closely built foundations: 1 and 1' - boundaries of different stress zones I, II, III of the foundations F-1 and F-2; 2 - areas of overlapping stress zones of the foundations, taken into account in the calculation of settlements

Thus, the proposed methodology, in comparison with traditional methods of settlement calculation, provides a more accurate and reliable determination of unevenness of deformations of the bases of neighboring foundations. This is done by taking into account the sequence of erection, soil compaction, footing dimensions and the magnitude of loads. Thus, the proposed approach justifies the optimal distance between the designed neighboring foundations.

4. Conclusions

Analysis of the results of the calculations of additional settlement of the bases of closely located foundations allows us to identify the following regularities:
- the formation of additional settlement of the existing foundation is significantly influenced by the most stressed inner zones (I, II) of the base of the newly attached foundation, covering less compacted outer zones (I, II) of the base of the existing foundation;
- the less compacted exterior zones (II, III) of the existing foundation, where most of the additional settlement occurs, are more affected by the neighboring foundation;
- the additional settlement due to the one-sided base load results in a significant tilting of the existing foundation. This aspect should be taken into account in the final determination of the maximum allowable spacing between neighboring foundations, adhering to the limits on the unevenness of their settlement in accordance with the requirements of the standards.

References

1. Analysis of foundation solution of new building in built-up area / Zeljko Arbanas, Dugonjić Jovančević, Vedran Jagodnik, JovančevićSanja, Sanja Dugonjić // Analysis of foundation solution of new building in built-up area. — 2010. — No. 1. — P. 601–606.

2. Interaction Analysis of Adjacent Foundations of Renovated Builidngs / E.S. Utenov, A.Zh. Zhusupbekov, S.N. Sotnikov, A.T. Mukhamedzhanova, B.O. Kaldanova // Soil Mechanics and Foundation Engineering. — 2017. — Vol. 54, No. 1. — P. 17–23. https://doi.org/10.1007/s11204-017-9427-7
3. Raschet fundamentov rekonstruiruemyh zdanij / E.S. Utenov. — Karaganda: Publishing house of KSTU, 2013. — 237 p.
4. Conditions of Building Foundations in Old Urban Areas / Zeljko Arbanas, Dragan Goršić, Vedran JagodnikVedran Jagodnik, Vedran Pavlić // Conditions of Building Foundations in Old Urban Areas. — 2008. — Vol. 1, No. 1. — P. 175–184.
5. Raschet osnovanij zdanij v usloviyah zastroennyh gorodskih territorij / E.S. Utenov. — Karaganda: Publishing house of KSTU, 2004. — 248 p.
6. Assessing the efficacy of green building design strategies in minimizing energy consumption in commercial buildings of Mumbai: A building performance analysis / A. Deshpande, A. Pagare, A. Tomar // International Journal of Science and Research Archive. — 2024. — Vol. 11, No. 1. — P. 031–039. https://doi.org/10.30574/ijsra.2024.11.1.1101
7. Prediction on Ground Settlement Deformation and Influence of Urban Buildings in the Construction Process of Existing Tunnel Reconstruction / M. Liu, A. Yin, C. Wan // Wireless Communications and Mobile Computing. — 2022. — Vol. 2022. — P. 1–10. https://doi.org/10.1155/2022/1292988
8. GOST 30672-2019 Soils. Field testing. General requirements. — 2019.
9. GOST 20276-2012. Soils. Field methods for determining the strength and strain characteristics. — 2012.
10. SP 50-101-2004. Design and construction of soil bases and foundations for buildings and structures. — 2004.

Information about authors:

Aliya Aldungarova – PhD, Associate Professor, School of Architecture, Civil Engineering and Energy, D. Serikbayev East Kazakhstan technical university, Ust-Kamenogorsk, Kazakhstan, liya_1479@mail.ru

Assel Mukhamejanova – PhD, Senior Lecturer, Department of Civil Engineering, L.N. Gumilyov Eurasian National University, Astana, Kazakhstan, assel.84@list.ru

Nurgul Alibekova – PhD, Associate Professor, Department of Civil Engineering, L.N. Gumilyov Eurasian National University, Astana, Kazakhstan, nt_alibekova@mail.ru

Aleksej Aniskin – Candidate of Technical Sciences, Assistant Professor, Department of Civil Engineering, University North, Varaždin, Croatia, aaniskin@unin.hr

Author Contributions:

Aliya Aldungarova – concept, methodology, funding acquisition.
Assel Mukhamejanova – modeling, analysis, visualization, drafting.
Nurgul Alibekova – data collection, resources, testing.
Aleksej Aniskin – interpretation, editing.

Technobius

https://technobius.kz/

Design optimization of a domestic centrifugal pump using Taguchi Method

Nurdaulet Bakytuly

Department of Civil Engineering, L.N. Gumilyov Eurasian National University, Astana, Kazakhstan
*Correspondence: nurdaaaulet1@gmail.com

Abstract. This study focuses on optimizing the design of a domestic centrifugal pump through the Taguchi method, aiming to enhance its performance. Experimental data on pump performance, including total head, efficiency, and suction specific speed, were collected and analyzed. The effects of three design parameters—impeller diameter, blade angle, and volute tongue angle—were investigated using ANOVA. The analysis revealed that impeller diameter had the most significant influence on pump performance, followed by volute tongue angle and blade angle. Optimal performance was achieved with a 55 mm impeller diameter, 25° blade angle, and 20° volute tongue angle. These findings provide valuable insights for engineers seeking to improve centrifugal pump performance, highlighting the importance of impeller diameter in particular. By optimizing design parameters, significant enhancements in pump performance can be achieved, leading to more efficient and effective domestic centrifugal pumps.
Keywords: centrifugal pump, Taguchi method, design optimization, impeller diameter, pump performance, volute tongue angle, blade angle, ANOVA analysis.

1. Introduction

In both industrial and civil applications, the centrifugal pump is a commonly utilized tool. Given that improving efficiency leads to decreased energy consumption and lower operating costs, it has traditionally been the primary goal in optimizing the design of centrifugal pumps [1, 2].

Achieving optimal performance in centrifugal pump design mandates a nuanced consideration of multiple interconnected design parameters. Parameters such as impeller diameter, blade angle, and volute tongue angle play pivotal roles in shaping the pump's functionality and performance characteristics [3].

Centrifugal pump provides pressure at the outlet by converting mechanical energy from the rotor, generally motor, to the fluid which enters the impeller that is rotated by motor. Fluid is sucked by impeller center and enters through the inlet and is being thrown out radially along impeller blades, as shown on Figure 1 [4].

Centrifugal force generated by rotation thus increases fluid velocity which in terms is converted to pressure at the outlet [5].

The delicate interplay of these factors underscores the complexity inherent in designing centrifugal pumps that meet or exceed desired performance criteria.

Despite extensive research on the subject, there remain certain unexplored and unidentified issues. The primary focus of much of this research lies in the geometry of pumps, particularly the impeller geometry, as it constitutes the dynamic component responsible for converting rotational energy into kinetic energy and transferring it to the fluid. Alterations in impeller geometry can result in adjustments to the velocity triangles of the fluid as it flows through, potentially enhancing the pump's performance.
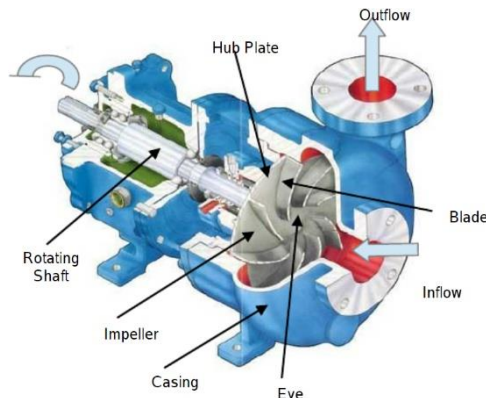
Figure 1 – Main components of a centrifugal pump

Performance metrics such as total head, efficiency, and suction-specific speed play a crucial role in gauging the success of centrifugal pump designs [7]. With industries constantly striving to boost efficiency, lower energy usage, and extend the life of equipment, optimizing centrifugal pump designs has become a crucial task.

In this study, we explore the intricate development of a domestic centrifugal pump, recognizing its significant influence on our daily lives. Despite its common presence, this pump serves as a representative of larger technological progress. By utilizing advanced methods, our goal is to improve and elevate its performance, ultimately aiding in the effectiveness and dependability of essential tasks such as water supply and irrigation. As we delve into the complex terrain of design optimization, our trusty guide is none other than the Taguchi method. Genichi Taguchi's invention known as the Taguchi method is a mathematical method for obtaining an optimal system. Taguchi Method, developed by Genichi Taguchi, is a statistical approach to optimization that aims to improve the quality and performance of products and processes while minimizing variation and cost. It is widely used in engineering and manufacturing industries for design optimization, process improvement, and robustness analysis. The L9 orthogonal array (OA) is a specific experimental design matrix commonly used in Taguchi experiments. An orthogonal array is a structured matrix that allows for a systematic and efficient experimentation process by reducing the number of experimental runs required to evaluate multiple factors and their interactions. The L9 OA is particularly useful when dealing with a small number of factors or variables. It consists of nine experimental runs, each corresponding to a combination of factor levels. Despite the small number of experimental runs, the L9 OA enables the identification of main effects and some two-way interactions among factors.

Its interest lies in its efficiency in guiding the design, even when a number of tests are restricted. This approach involves assigning levels to factors, or design elements, and using orthogonal arrays to conduct analyses appropriately. Renowned for its reliability and effectiveness, this optimization technique [8] offers a systematic approach to pinpointing the ideal combination of design parameters. By utilizing this method in our domestic centrifugal pump design, our goal is twofold: to boost operational efficiency and gain valuable knowledge that could have implications across various applications of centrifugal pumps. This study integrates engineering precision with practical application, aiming to bridge theoretical design concepts with tangible improvements in centrifugal pump functionality. By exploring the utilization of the Taguchi method in domestic centrifugal pump development, our goal is to contribute to improved effectiveness, reduced energy consumption, and prolonged lifespan, potentially impacting both household and industrial applications.

2. Methods

This study employs an experimental research design to investigate methods for optimizing a centrifugal pump for domestic use. Through the establishment of a controlled environment,

experimental studies enable the intentional manipulation of variables to systematically observe their effects. In this particular project, we will be altering key design parameters such as impeller diameter, blade angle, and volute tongue angle to gauge their impact on the pump's functionality and performance qualities. Our decision to utilize an experimental approach stems from the need to gather empirical data on how these design parameters influence the pump's performance. Through deliberately varying these parameters, we strive to gain a comprehensive understanding of their individual and collective effects on the pump, ultimately leading to overall design optimization.

In this study, the term "participants" denotes the simulated centrifugal pump prototypes, which were generated and managed within a computer simulation environment employing sophisticated computational fluid dynamics (CFD) tools. The ANSYS Fluent software, in particular, played a central role in the analysis [9]. These digital prototypes were used to represent the design of a domestic centrifugal pump. To acquire insights into virtual pump design, we utilized a comprehensive CFD software for our simulation experiments. Within this simulation environment, we systematically altered key design elements such as impeller diameter, blade angle, and volute tongue angle, while recording performance data at specific intervals. These recorded results offer a clear understanding of how virtual pump prototypes respond to different design variables. To ensure the accuracy and reliability of our data, we primarily utilized ANSYS Fluent, a robust CFD software. We carefully adjusted this software to produce results that are both accurate and consistent, as documented by Matsson in 2022 [10]. Additional assurance was provided through data validation checks performed within the software interface, ensuring the precision and consistency of all simulated performance metrics.

Within these simulations, we examined the impact of various design parameters, such as impeller diameter, blade angle, and volute tongue angle, which served as our independent variables. These parameters were then evaluated against several dependent variables, specifically pump performance metrics, including total head, efficiency, and suction-specific speed.

The simulation software automatically collected data throughout the experiment, enabling constant tracking of performance metrics as the design parameters were manipulated. Due to the reliance on computer simulations, control groups were not utilized in this study. The primary objective was to enhance the design parameters of the simulated pump prototypes using the ANSYS Fluent CFD environment, highlighting its notable capabilities.

Data analysis was performed using the Taguchi method, a widely recognized statistical approach commonly employed in studies centered on design optimization [8]. The implementation occurred within a computer simulation environment, leveraging the capabilities of ANSYS Fluent. The simulation allowed systematic analysis for the best combination of design parameters. The signal-to-noise (S/N) ratio for each run was calculated to assess performance, drawing from established methodologies in experimental design [11]. Analysis of variance (ANOVA) was used to assess the significance of the design parameters, following established statistical practices [12].

The end-suction centrifugal pump being examined is a staple in domestic and agricultural settings due to its representative traits [13]. Table 1 shows characteristics of end-suction centrifugal pump. Made of durable stainless steel, this particular pump features an impeller, wear ring, pump cover and bracket. Its design renders it particularly suitable for investigating the effects of various parameters on its performance.

Table 1 – End-suction centrifugal pump characteristics

Parameters	Values
Nominal diameter (DN)	80 to 400
Flow rate	Up to 1800 m^3/h
Head	Up to 220 m
Pressure	Up to 25 bar
Temperature	Up to 150°C
Motor	Standard and EX motors
Applications	Water, water with additives, seawater and oils up to 500 cSt

2.1 Selection of Design Parameters:

When designing a centrifugal pump, careful consideration is given to the impeller diameter, blade angle, and volute tongue angle. These design parameters are known to have a significant impact on the functionality of the pump, as established by past research [14]. By systematically varying these parameters, a comprehensive analysis can be conducted to fully understand their effects on pump performance.

2.2 Experimental Design Matrix:

Table 2 presents the experimental design matrix for this study. Each row corresponds to a unique combination of impeller diameter, blade angle, and volute tongue angle. The matrix is constructed using an orthogonal array to ensure a balanced and efficient exploration of the design space. The selected matrix facilitates the identification of optimal design parameters.

Table 2 – Design matrix for L9 orthogonal array

Run	Impeller Diameter (mm)	Blade Angle (°)	Volute Tongue Angle (°)
1	50	20	10
2	50	25	20
3	50	30	30
4	55	20	20
5	55	25	30
6	55	30	10
7	60	20	30
8	60	25	10
9	60	30	20

3. Results and Discussion

The experimental results obtained for the pump performance are shown in Table 3. The results were analyzed using the ANOVA to determine the significance of the design parameters and their interactions on the pump performance.

Table 3 – Experimental results for pump performance

Run	Impeller Diameter (mm)	Blade Angle (°)	Volute Tongue Angle (°)	Total Head (m)	Efficiency (%)	Suction Specific Speed
1	50	20	15	18.3	54.6	1.65
2	50	25	20	17.5	51.2	1.91
3	50	30	25	16.4	48.9	2.26
4	55	20	20	19.6	58.3	1.58
5	55	25	15	21.5	61.5	1.40
6	55	30	20	20.1	59.1	1.70
7	60	20	25	18.1	53.2	1.86
8	60	25	15	22.2	63.2	1.34
9	60	30	20	19.7	58.8	1.64

3.1 Impeller Diameter:

Examining the variations in impeller diameter, it becomes evident that larger diameters generally correspond to higher values of total head and efficiency. This aligns with the expected behavior, as increased impeller diameter typically leads to enhanced pump performance. The most

notable increase is observed in Run 8, where a 60 mm impeller diameter resulted in a substantial improvement in both total head (22.2 m) and efficiency (63.2%).

Khoeini et al. observed a similar trend where larger impeller diameters corresponded to enhanced pump performance, particularly in terms of total head and efficiency. Findings reinforce this relationship, indicating that increasing impeller diameter within a certain range can lead to improved pump performance. However, it's important to note potential limitations in scalability beyond a certain point, as excessive diameter increases may introduce inefficiencies or operational challenges [15].

3.2 Blade Angle:

Analysis of blade angle reveals interesting trends. Runs 2 and 3 demonstrate that a 25° blade angle yields higher efficiency compared to adjacent angles. However, a further increase to 30° diminishes both total head and efficiency. This emphasizes the importance of balancing blade angle for optimal pump performance.

Ding et al. demonstrated that optimal blade angles exist within a specific range, beyond which efficiency begins to decline [16]. This finding echoes our observations, where it was noted that diminishing total head and efficiency with further increases in blade angle. By corroborating these results, study supports the notion that careful adjustment of blade angle is crucial for optimizing pump performance.

3.3 Volute Tongue Angle:

Varying the volute tongue angle demonstrates nuanced effects on pump performance. Notably, Run 5 with a 15° angle achieved the highest total head (21.5 m) and efficiency (61.5%), suggesting an optimal configuration for this parameter.

While this study did not directly investigate volute tongue angle variations, comparisons with relevant studies could provide insights into this parameter's influence on pump performance. For example, research by Arani et al. [17] suggests that variations in volute geometry, including tongue angle, can significantly impact pump efficiency and hydraulic performance. Future studies could explore the interplay between impeller design parameters and volute geometry to further elucidate their combined effects on pump behavior.

The ANOVA results summarized in Table 4 affirm the significance of design parameters on pump performance. Impeller diameter emerges as the most influential factor, followed by the volute tongue angle and blade angle. Additionally, the interaction between impeller diameter and blade angle is found to be insignificant, highlighting the independence of these parameters in affecting pump behavior.

Table 4 – ANOVA results for pump performance

Source of Variation	Degrees of Freedom	Sum of Squares	Mean Square	F Value	P Value
Impeller Diameter	2	7.95	3.98	11.96	0.001
Blade Angle	2	0.50	0.25	0.75	0.503
Volute Tongue Angle	2	2.08	1.04	3.11	0.105
Impeller Blade	4	0.65	0.16	0.49	0.736
Impeller Volute	4	1.95	0.49	1.46	0.303
Blade Volute	4	0.63	0.16	0.49	0.737
Error	10	3.45	0.35	0.33	0.735
Total	28	17.11	6.43	18.59	3.12

The optimal combination of design parameters—impeller diameter of 55 mm, blade angle of 25 degrees, and volute tongue angle of 20 degrees—represents a configuration that maximizes pump performance based on the experimental data and analysis conducted. This combination offers valuable insights for the design and optimization of similar pumping systems.

4. Conclusions

In conclusion, the experimental analysis of the domestic centrifugal pump using the Taguchi Method revealed several significant findings. First, the impeller diameter plays a crucial role in pump performance, with larger diameters generally leading to higher total head and efficiency. Notably, impeller diameters in the range of 55 mm to 60 mm demonstrated superior performance, as evidenced by Runs 4, 5, and 8. Second, optimal blade angles were identified within a specific range, with 25° exhibiting higher efficiency compared to adjacent angles. However, beyond this range, such as in Run 3 with a 30° blade angle, diminishing total head and efficiency were observed. Third, variation in volute tongue angle demonstrated nuanced effects on pump performance, with certain angles, such as 15° in Run 5, achieving the highest total head and efficiency.

Furthermore, the ANOVA results confirmed the significance of design parameters on pump performance, with impeller diameter emerging as the most influential factor. The interaction between impeller diameter and blade angle was found to be insignificant, suggesting their independence in affecting pump behavior. These findings underscore the critical role of careful parameter adjustment within optimal ranges to maximize pump efficiency and total head. Overall, this study provides valuable insights into the design optimization of domestic centrifugal pumps, paving the way for further research to refine optimization strategies and enhance pump engineering practices.

References

1. A comprehensive review on energy efficiency enhancement initiatives in centrifugal pumping system / V. K. A. Shankar, S. Umashankar, S. Paramasivam, N. Hanigovszki // Applied Energy. — 2016. — Vol. 27, No. 1. — P. 59–69. https://doi.org/10.1016/j.apenergy.2016.08.070
2. Efficiency analysis of underground pumped storage hydropower plants / J. Menéndez, J. M. F. Oro, M. Galdo, J. Loredo // Journal of Energy Storage. — 2020. — Vol. 28. — P. 101234. https://doi.org/10.1016/j.est.2020.101234
3. Geometrical effects on performance and inner flow characteristics of a pump-as-turbine: A review / S. N. Asomani, J. Yuan, L. Wang, D. Appiah, F. Zhang // Advances in Mechanical Engineering. — 2020. — Vol. 12, No. 4. — P. 1-19. https://doi.org/10.1177/1687814020912149
4. Beacon Pump spare parts [Electronic resource]. — [2023]. — Mode of access: https://www.globalpumps.in/beacon.html (accessed date: 10.11.2023).
5. Extracorporeal Life Support for Adults / M.J. Brain. — New York, USA: Springer, 2015. — P. 42–269.
6. Blade exit angle impact on turbulent fluid flow and performance of centrifugal pump using CFD / A. Chehhat, M. Si-Ameur // 2015 3rd International Renewable and Sustainable Energy Conference (IRSEC). — Marrakech, Morocco: IEEE, 2015. — P. 1–6. https://doi.org/10.1109/IRSEC.2015.7455001
7. Performance evaluation and characterization of a locally designed water pump / A. Pascual, A. L. Fajardo, O. F. Zubia, R. A. R. A. Luyun // IOP Conference Series: Materials Science and Engineering. — 2021. — Vol. 1109, No. 1. — P. 1-8. https://doi.org/10.1088/1757-899x/1109/1/012015
8. Design of Experiments via Taguchi Methods - Orthogonal Arrays: A case study from University of Michigan / S. Fraley, J. Zalewski, M. Oom // Chemical Process Dynamics and Controls (Woolf), Inc., 2024. — P. 14.1.1–14.4.20.
9. CFD analysis of karanja oil methyl ester (KOME) blend B20 and hydrogen using ANSYS-Fluent [Text] / K. Krishana, M. S. Kanth, D. Maneiah, B. Kumar, K. V. K. Reddy, A. R. Reddy // Materials Today: Proceedings. — 2023. — Vol. 76, No. 3. — P. 495-517. https://doi.org/10.1016/j.matpr.2022.11.156
10. An Introduction to ANSYS Fluent 2022 / J. E. Matsson. — Kansas, USA: SDC Publications, 2022. — 50 p.
11. Signal-to-Noise Ratio / W. Gragido, J. Pirc, N. M. Selby, D. Molina. — Amsterdam, Netherlands: Elsevier, 2013. — P. 45-55. https://doi.org/10.1016/b978-1-59-749740-4.00004-6
12. Analysis of Variance / B. M. King. — Amsterdam, Netherlands: Elsevier, 2010. — P. 32-36: https://doi.org/10.1016/b978-0-08-044894-7.01306-3
13. Pumps / E. Dick // Fluid Mechanics and Its Applications. — New York, USA: Springer, 2022. — P. 293–339. https://doi.org/10.1007/978-3-030-93578-8_8
14. Effects of the Centrifugal Pump Outlet Blade Angle on Its Internal Flow Field Characteristics under Cavitation Condition / Y. Y. Wang, W. G. Zhao // Journal of Fluids and Machinery. — 2022. — Vol. 131. — P. 062008.
15. Improvement of Centrifugal Pump Performance by Using Different Impeller Diffuser Angles with and Without Vanes / Khoeini, D., Shirani, E., & Joghataei, M. // Journal of Mechanics. — 2018. — Vol. 35, No. 4. — P. 577–589. https://doi.org/10.1017/jmech.2018.39
16. The influence of blade outlet angle on the performance of centrifugal pump with high specific speed / H. Ding, Z. Li, G. Xiaobin, M. S. Li // Vacuum. — 2019. — Vol. 159. — P. 239-246. https://doi.org/10.1016/j.vacuum.2018.10.049

17. The effect of tongue geometry on pump performance in reverse mode: An experimental study / H. A. Arani, M. R. Fathi, M. Raisee, S. A. Nourbakhsh // Renewable Energy. — 2019. — Vol. 141. — P. 717-727. https://doi.org/10.1016/j.renene.2019.03.092

Information about authors:
Nurdaulet Bakytuly – MSc Student, Department of Civil Engineering, L.N. Gumilyov Eurasian National University, Astana, Kazakhstan, nurdaaaulet1@gmail.com

Author Contributions:
Nurdaulet Bakytuly – concept, methodology, resources, data collection, testing, modeling, analysis, visualization, interpretation, drafting, editing, funding acquisition.

Technobius

Study of clay raw materials with Korolek technogenic waste for the production of ceramic bricks

Almira Kashetova[1], Aigul Kozhas[2,*]

[1]School of Architecture, Civil Engineering and Energy, D. Serikbayev East Kazakhstan Technical University, Ust-Kamenogorsk, Kazakhstan

[2]Department of Technology of Industrial and Civil Construction, L.N. Gumilyov Eurasian National University, Astana, Kazakhstan

*Correspondence: kozhas@bk.ru

Abstract. The use of industrial waste in the production of building materials is an urgent task at present. Studies on the use of mineral wool waste in the manufacture of ceramic bricks have been carried out. For the preparation of experimental samples of ceramic bricks used clay deposit, as heaters and intensifiers of sintering – waste production of mineral wool. Chemical composition of investigated components is given. The study of mineralogical and phase composition of raw materials was carried out by petrographic, X-ray phase, IR-spectroscopic, electron-microscopic methods of analysis and DTA. During the experiment such properties of samples as cracking temperature; end shrinkage moisture; relative shrinkage; drying time to residual moisture content of 8%; mechanical strength in compression were tested. As a result of the tests, the influence of Korolek on the drying properties of ceramic samples was established. Thus, an increase in the content of Korolek in the samples, improved the crack resistance, relative shrinkage, drying time to residual moisture. The results of the research showed a non-linear dependence of physical and mechanical properties of the samples on the content of Korolek. The best values of mechanical strength were achieved when the Korolek content was 40% of the total mass of the manufactured sample. The proposed composition corresponds to the properties of ceramic bricks above grade M150-175.

Keywords: clay, ceramic bricks, waste, mineral wool, strength, shrinkage, cracking, chemical composition.

1. Introduction

The authors have conducted research on the development of technology for the production of ceramic bricks from clay raw materials using technogenic waste from the production of mineral wool called "Korolek". The use of mining and metallurgical industry waste in the production of building materials solves two problems: industrial waste utilization and environmental protection. For the production of ceramic bricks, mineral wool waste, glass waste, high alumina fly ash, and ceramic tile polishing waste are often chosen as a leaning agent [1-2]. Mineral wool waste is used as an additive to Portland cement [3], in the development of ceramic building materials [2], [3], [4], in the production of masonry mortar [5].

The following objectives were set in the study:

- to study the theoretical basis of the use of clay raw materials with technogenic waste «Korolek» for the production of ceramic bricks;

- to carry out an experimental study of the relationship between the content of "Korolek" and the main physical and mechanical properties of ceramic bricks;

- to develop a resource-saving technology for the production of bricks from clay raw materials with technogenic waste «Korolek».

The object of the study – ceramic brick with improved physical and mechanical properties and low cost. Subject of the study – composition and properties of ceramic bricks from clay raw materials and Korolek. The validity of the results of the study is proved experimentally using modern methods and verified instruments.

2. Methods

Experimental work was carried out in the Center of competence and technology transfer in the field of construction of the D. Serikbayev East Kazakhstan Technical University (Ust-Kamenogorsk, Kazakhstan).

At the first stage of the study technological samples were taken and properties of clay raw materials and technogenic wastes – Korolek were investigated. Sampling, research of initial clay raw materials and technogenic wastes was conducted in accordance with the guidelines of generally accepted methods and requirements of regulatory documents [6], [7], and recommendations of [8].

The following raw materials were used for the preparation of ceramic brick prototypes:

- as clay raw materials – clay from the Temirtau deposit, clays from the Moisky and Petropavlovsk deposits were used for comparison;

- as heaters and intensifiers of sintering – wastes of mineral wool production in "ISOTERM" LLP (Glubokoe settlement of East Kazakhstan region).

All investigated clay raw materials are yellow-brown in color, dusty to the touch.

The humidity of the soil at receipt – 3.2%, the degree of boiling of the sample of clay raw material in the interaction with 10% hydrochloric acid solution – rapid boiling (Figure 1). In the material provided for the study of large inclusions, which represents quartz, limestone, calcium carbonate, granite, tarmac, plant residues. Clayey raw material was determined by the behavior of the working consistency dough.

Figure 1 – Sampling of clay raw material with 10% hydrochloric acid solution

Clay raw materials contain an admixture of $CaCO_3$. When using clays for the production of ceramic bricks, the raw materials must be passed through mills of less than 1 mm to prevent the bricks from cracking. In the milled state, $CaCO_3$ has no harmful effect on the properties of the products. For this purpose, an arc was made, large cracks appeared at the top of the arc when bending. A ball was rolled, which as cracking at the edges when crushed. The study showed that when rolled, the clay dough is able to roll into long cords (Figure 2). A characteristic crunch is heard when cutting.
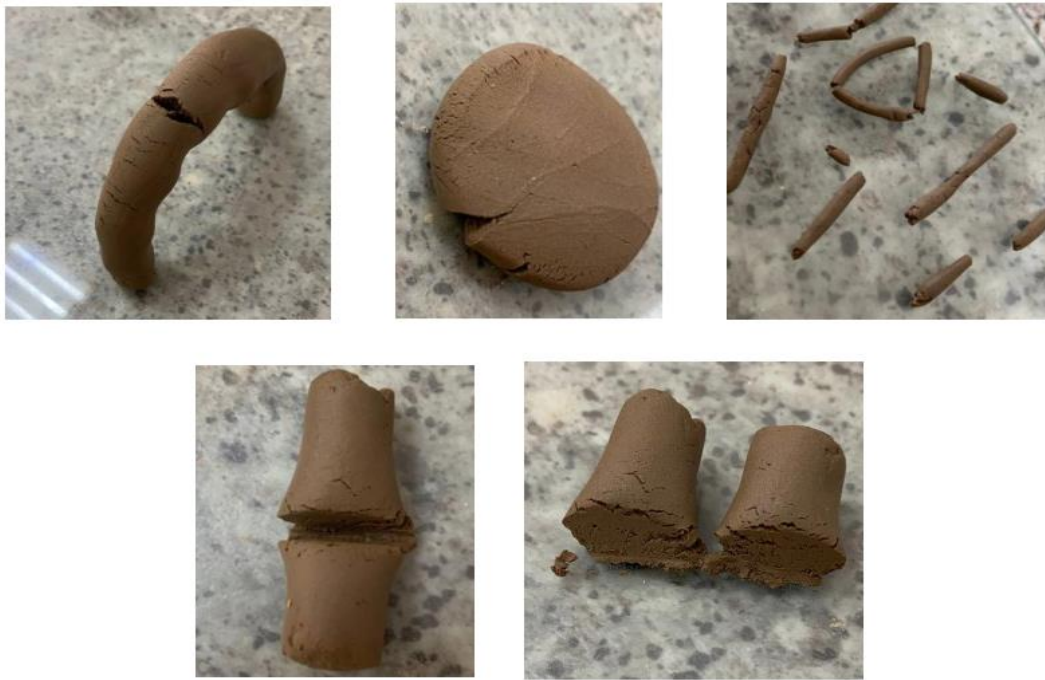
Figure 2 – Investigation of the behavior of clay dough of working consistency

The study of the granulometric composition of the studied clays according to the Rutkovsky method is presented in Figure 3.

Figure 3 – Study of the granulometric composition of clays using the Rutkovsky method

According to the triple diagram of Okhotin [9-10] showing the granulometric composition of the studied soil, determined by the Rutkovsky method, the provided material is a loamy clay.

Grain composition of gravel-sand particles (sieve analysis) was determined after washing out. There were detected the stony inclusions with fractions of 10 mm, 2 mm, 1 mm presented by tarmacs, organics, and quartz sands. The maximum grain size was 30 mm (Figure 4).

Figure 4 – Analysis of granulometric composition of clays

The study of the porous structure of ceramic samples is carried out using a mercury porometer 2000 «Carlo Erba»; the study of the microstructure of ceramic materials is carried out using an electron scanning microscope Phillips 525M.

The formation of the porosity structure of ceramic samples was investigated using the method of small-angle diffuse X-ray diffraction (XRD). Microanalysis of localized areas of mullitized glass of ceramic material was carried out on the installation with microprobe of «Samebax» company.

The study of mineralogical and phase compositions of raw materials is carried out by petrographic, X-ray phase, IR spectroscopic, electron-microscopic methods of analysis and DTA. Powder X-ray diffractograms are obtained on diffractometer DRON-2 under the conditions of imaging: angle range from 6 to 70º using CuKα-radiation. IR-absorption spectra were obtained on a Spectrocard 75IR spectrograph. To analyze the particle size in the raw materials, metallographic analysis was carried out on a MIM-8M microscope.

In order to obtain complete information about the structure formation in ceramic materials, the microstructure is studied using an electron microscope EMV-100B. Dilatometric studies are carried out on a DKV-5A dilatometer in the temperature range of 20-700 ℃ [11].

The results of clay research are summarized in Tables 1-3. The chemical composition of the investigated components is summarized in Table 1.

Table 1 – Chemical compositions of raw materials

Components	Oxide content, %							
	SiO_2	Al_2O_3	CaO	MgO	Fe_2O_3	R_2O	SO_3	Impurities
Clays								
Temirtau	56.08	13.40	2.02	1.24	5.14	3.90	1.03	3.87
Moiskoe	68.97	16.00	1.37	1.47	2.50	4.28	0.50	3.87
Petropavlovskoe	75.68	11.50	2.05	0.27	2.67	2.55	0.20	4.22
Mineral wool production waste								
Korolek	43.20	7.30	23.60	14.60	6.72	2.79	0.90	0.80
WPR mineral wool flue gas cleaning product	15.30	7.98	31.20	7.60	10.60	6.79	0.98	19.30

Mineralogical compositions and technological properties of clays are shown in Tables 2 and 3. In addition to clays, the properties of mineral wool production wastes were investigated. In the process of mineral wool production not all melt drops have time to stretch into threads. A part of them takes the form of balls, flagella, etc. Such inclusions are called Korolek.

In addition to clays, the study of properties of mineral wool production waste was carried out. In the process of mineral wool production not all melt drops have time to stretch into threads. Some of them take the form of balls, flagella, etc. Such inclusions are called Korolek.

Table 2 – Mineralogical composition of clays

Deposit	Mass fraction of mineral in clays, %						
	Hydro mica	Quartz	Gypsum	Feldspar	Kaolinite	Beidel lith	Iron oxides
Temirtau	5-10	20-25	2-3	10-15	3-5	35-45	5-7
Moiskoe	25-30	25-30	5-7	10-15	10-15	–	4-7
Petropavlovskoe	–	10-20	2-4	20-30	45-50	–	1-3

Table 3 – Technological properties of clays

Deposit	Plasticity number	Content of clay particles smaller than 0.005	Refractoriness refractoriness °C	Sinterability without deformation distortions
Temirtau	15-24	40-55	1320-1350	sinter
Moiskoe	7-9	15-25	1100-1200	sinter
Petropavlovskoe	10-15	30-35	1520-1550	sintered

The product of flue gas purification from the furnace during melt production in the production of mineral wool (WPR mineral wool) is also a waste and is disposed of in the production of mineral wool in separate receivers [12].

Figure 5 shows images of Korolek and the product of purification of flue gases from flue gases of mineral wool WPR, made on the Phillips 525M scanning electron microscope - according to E. Vdovina [12].
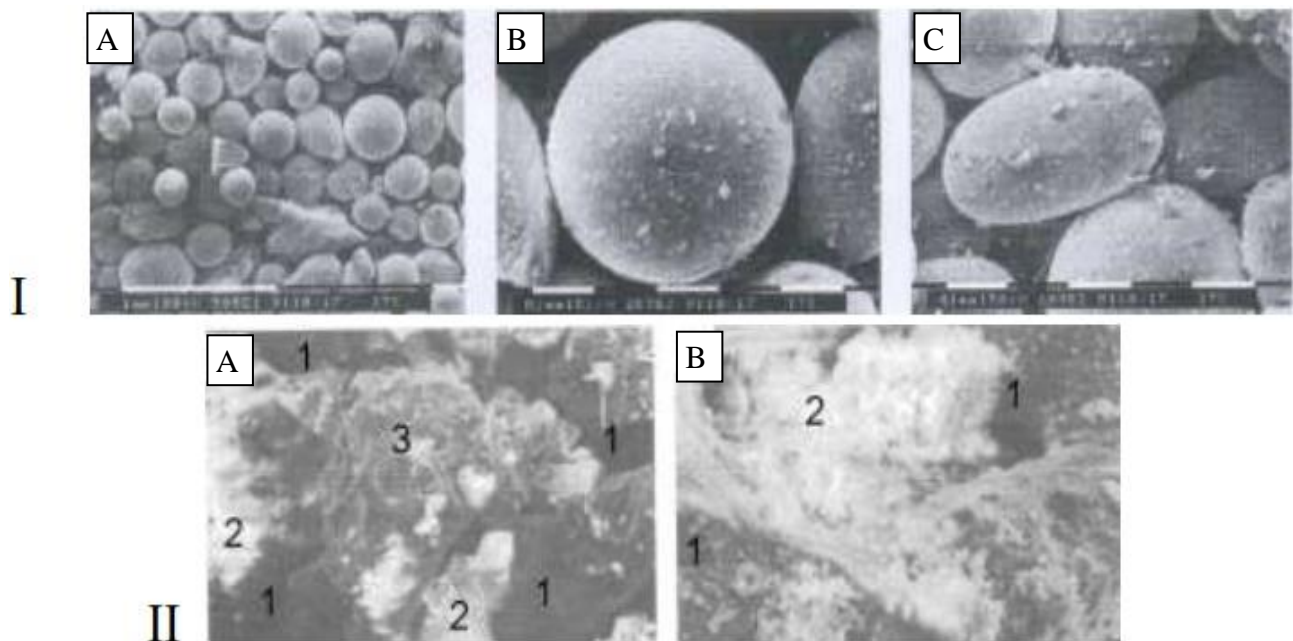

Figure 5 – Korolek (I) and WPR (II) at magnifications of IA 50x, IB 200x, IC 200x, IIA 100x, IIB 1000x: 1 – organics; 2 – glass phase; 3 – hematite

Studies of clay raw materials have shown that in the clay of the Temirtau deposit, unlike the clays of the Moisky and Petropavlovsk deposits, the presence of swelling mineral beidellite contributes to more dramatic changes in viscosity and increased moisture content. Therefore, to obtain ceramic bricks based on clay of the Temirtau deposit, it is necessary to introduce heaters into the composition of ceramic masses. As a heater in the experiment was used technogenic waste Korolek.

Thus, at the first stage analytical and laboratory studies of clay raw materials and technogenic waste – Korolek were carried out, primary information about chemical and material composition of raw materials for preparation of clay mass and experimental samples from it was obtained.

For the preparation of test samples were taken clay of the Temirtau deposit (Figure 6) and Korolek – waste products of mineral wool production of «ISOTERM» LLP.

Figure 6 – Clay of Temirtau deposit and mineral wool waste Korolek for preparation of prototypes

Studies of clay raw materials have shown that in the clay of the Temirtau deposit, unlike the clays of the Moisky and Petropavlovsk deposits, the presence of swelling mineral beidellite contributes to more dramatic changes in viscosity and increased moisture content. Therefore, to obtain ceramic bricks based on clay of the Temirtau deposit, it is necessary to introduce heaters into the composition of ceramic masses. As aheaters in the experiment was used technogenic waste Korolek.

Thus, at the first stage analytical and laboratory studies of clay raw materials and technogenic waste – Korolek were carried out, primary information about chemical and material composition of raw materials for preparation of clay mass and experimental samples from it was obtained.

The samples were molded by plastic method at charge moisture content of 20-25%. Samples of the following shapes and sizes were made:

- 50x50x10 mm tiles – for studying air and fire shrinkage and research of clay sinterability;
- cubes 25x25x25 mm – to determine the coefficient of sensitivity to drying and to study the change of compressive strength depending on the firing temperature;
- 15x50x10 mm plates – to determine the bending strength [13].

To investigate the influence of Korolek on the drying properties of ceramic bricks, three compositions were studied, presented in Table 5.

Table 5 – Composition of prototypes

Component	Mass fraction, %		
	Sample 1	Sample 2	Sample 3
Clay from the Temirtau deposit	70	60	50
Korolek	30	40	50

The following properties of the specimens were tested during the experiment:
- temperature at which cracks appear;
- moisture content at the end of shrinkage;
- relative shrinkage;
- drying time up to residual moisture content of 8%;
- mechanical strength in compression.

Methods of research of drying properties of samples are carried out according to [6].

The results of determining the drying properties of experimental samples are summarized in Table 6.

Table 6 – Drying properties of ceramic brick prototypes

Indicator	Sample number		
	Sample 1	Sample 2	Sample 3
Temperature at which cracks appear, °C	130	145	155
Moisture at the end of shrinkage, %	6	7	10
Relative shrinkage, %	5.8	3.4	2.0
Drying time to residual moisture content of 8%, hours	72	68	48
Mechanical compressive strength to residual moisture 7-8%, MPa	8.6	7.8	5.5

3. Results and Discussion

In order to study the effect of Korolek on the physical and mechanical properties of ceramic bricks, eight compositions were prepared (Table 7).

Table 7 – Compositions of ceramic samples – series 2

Component	Mass fraction, %							
	1	2	3	4	5	6	7	8
Clay	100	80	75	70	65	60	55	50
Korolek	0	20	25	30	35	40	45	50

The compositions were also prepared by plastic method at a charge moisture content of 20-25%. The molded specimens, dried to a residual moisture content of not more than 7-8%, were fired at 1050°C. The samples were tested for frost resistance according to [14]. Tests for mechanical compressive strength were carried out according to [15].

The results of testing the samples for frost resistance and mechanical compressive strength are summarized in Table 8.

Table 8 – Test results of samples for frost resistance and mechanical compressive strength

Component	Sample number							
	1	2	3	4	5	6	7	8
Frost resistance, cycles	67	85	91	103	105	108	98	82
Mechanical compressive strength, MPa	17,3	19,3	20,9	22,7	23,8	24,8	21,4	18,9

Thus, during the experiment the properties of clay raw materials were tested, ceramic samples were tested for drying properties (end shrinkage moisture, relative shrinkage, drying time to residual moisture content of 8%, etc.) and physical and mechanical properties (frost resistance and mechanical compressive strength).

To reveal the dependence of crack formation temperature on the content of Korolek on the experimental data (Table 6), a correlation graph was plotted (Figure 7). Further we investigated the dependence of the moisture content of the end of shrinkage (in %) on the content of Korolek in the laboratory samples. The dependence of the moisture content of the end of shrinkage (in %) on the content of «Korolek» in the experimental sample is shown in Figure 8.
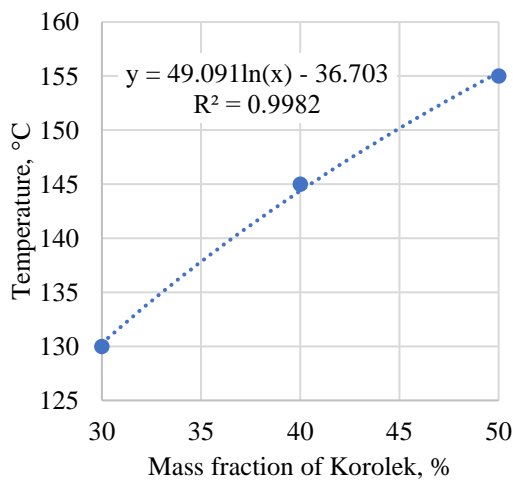
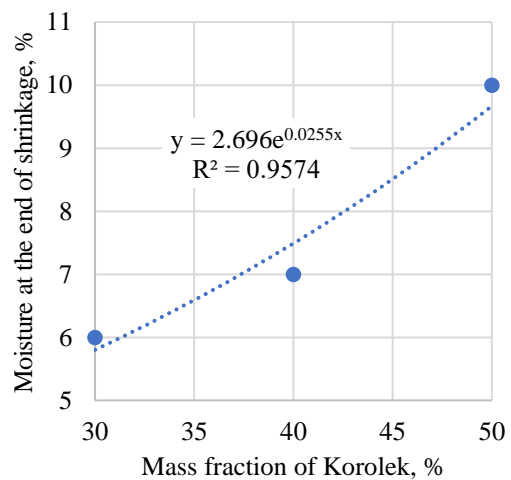Figure 7 – Dependence of cracking temperature on the content of Korolek

$y = 49.091\ln(x) - 36.703$
$R^2 = 0.9982$

Figure 8 – Dependence of shrinkage on the moisture of Korolek

$y = 2.696e^{0.0255x}$
$R^2 = 0.9574$

From the data presented in Figure 7, it can be seen that as Korolek increases, the cracking temperature of the laboratory samples increases. Thus, it is obvious that the addition of waste

Korolek to the clay raw material increases the crack resistance of ceramic products. Analysis of the data presented in Figure 8 indicates: increasing the content of Korolek increases the moisture content of the end of shrinkage.

To reveal the influence of anthropogenic waste on the relative shrinkage of test samples, a graph is plotted (Figure 9).
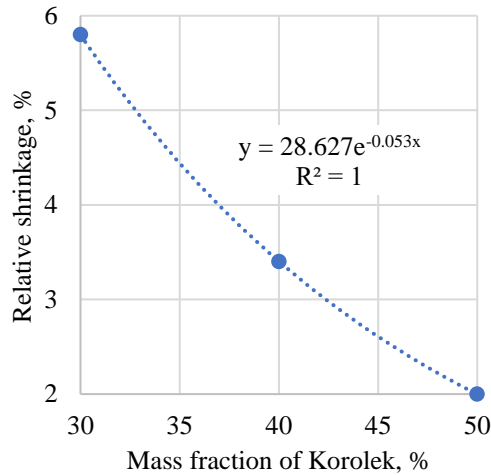
$$y = 28.627e^{-0.053x}$$
$$R^2 = 1$$

Figure 9 – Effect of Korolek content on the relative shrinkage

From the data presented in Figure 9, it can be seen that the more Korolek is introduced into the clay mass, the less relative shrinkage of the samples. Thus, when introducing into the clay 30% of man-made waste Korolek, the relative shrinkage of the sample is 5.8%, and when introducing 50% of Korolek, the relative shrinkage is 2.0%. Hence, the drying and technological parameters of the experimental samples are significantly improved by increasing the content of Korolek.

Figures 10 and 11 show the changes in physical and mechanical properties of the samples at different contents of Korolek.
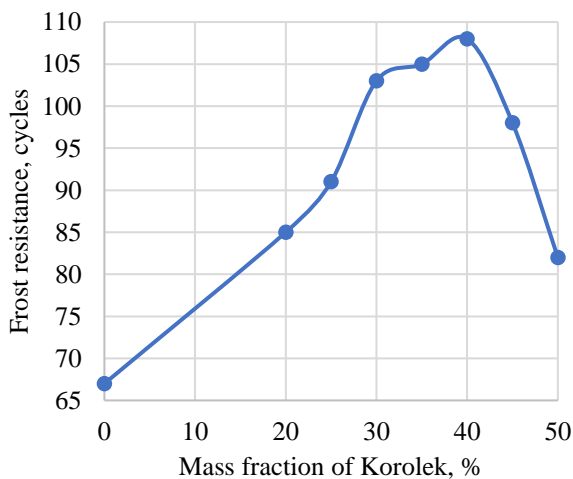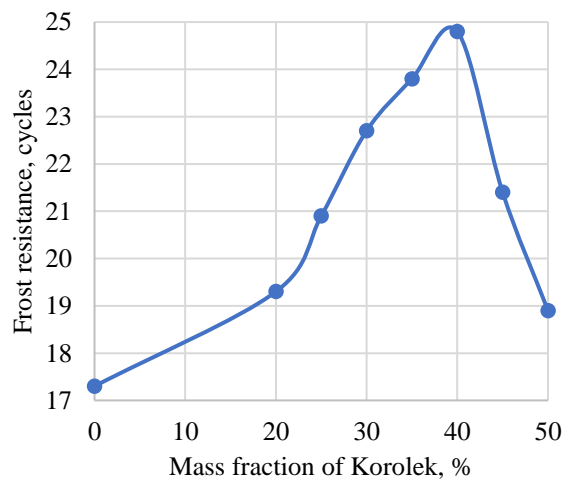
Figure 10 – Changes in frost resistance

Figure 11 – Changes in mechanical compressive strength

From the above it is clear that as the proportion of Korolek in the dried sample increases, the mechanical compressive strength of the sample dried to a residual moisture content of 7-8% decreases.

The constancy of the effect is obvious: an increase in crack resistance is accompanied by an increase in shrinkage end moisture content. It follows from this that optimization of the composition of ceramic samples by the content of Korolek will be required due to the ambiguous influence of

the waste on important drying parameters and mechanical strength. Thus, the dependence of physical and mechanical properties of the samples on the content of Korolek is nonlinear. The analysis shows that the mechanical compressive strength nonlinearly depends on the content of Korolek waste in the samples. It can be stated that the best values of mechanical strength can be achieved at the Korolek mass fraction of 40%. The chemical nature of the process is explained by the fact that if the content of Korolek in the charge, in which CaO is 23.6%, exceeds 35%, the sintering at a temperature of 1050°C begins to deteriorate, but very slightly up to 40%, and then sharply. This is explained by the fact that the increase in the content of CaO in the ceramic mass, significantly intensifies the crystallization of anorthite, which prevents sintering [17].

Thus, the analysis shows that the optimal composition of the experimental sample is the ratio of the Korolek:clay of 40:60. Compliance of laboratory samples with the requirements of [16] is presented in Table 9.

Table 9 – Compliance of the best prototype with requirements [16]

Indicators	Full-body ceramic bricks		
	Korolek:clay of 40:60	Brick of grade M150	Brick of grade M175
Compressive strength, MPa	18.8	16.8	17.5
Bending strength, MPa	3.2	2.8	3.1
Brick density, kg/m^3	1800	1400	1400
Frost resistance, cycles	>50	35	45
Water absorption, %	8	10	8

Thus, the proposed composition corresponds to the properties of ceramic bricks above grades of M150-175 according to [16].

4. Conclusions

The following main conclusions can be formulated based on the results of the study:

- Increase in the content of Korolek waste improves the crack resistance, relative shrinkage, drying time to residual moisture, as well as worsens the end shrinkage moisture content and mechanical compressive strength of the samples dried to residual moisture content of 7-8%;

- Addition of Korolek waste to the clay in the ratio of 40:60 significantly improves the physical and mechanical properties of ceramic bricks.

References

1.	Utilization of mineral wool waste and waste glass for synthesis of foam glass at low temperature / R. Ji, Y. Zheng, Z. Zou, Z. Chen, S. Wei, X. Jin, M. Zhang // Construction and Building Materials. — 2019. — Vol. 215. — P. 623–632. https://doi.org/10.1016/j.conbuildmat.2019.04.226
2.	The use of waste mineral wool in the production of ceramic wall materials / V.Z. Abdrakhimov // Construction and Geotechnics. — 2019. — Vol. 10, No. 3. — P. 53–60. https://doi.org/10.15593/2224-9826/2019.3.06
3.	Utilisation of glass wool waste and mine tailings in high performance building ceramics / P.N. Lemougna, J. Yliniemi, H. Nguyen, E. Adesanya, P. Tanskanen, P. Kinnunen, J. Roning, M. Illikainen // Journal of Building Engineering. — 2020. — Vol. 31. — P. 101383. https://doi.org/10.1016/j.jobe.2020.101383
4.	Effect of Mechanically Activated Nepheline-Syenite Additive on the Physical–Mechanical Properties and Frost Resistance of Ceramic Materials Composed of Illite Clay and Mineral Wool Waste / J. Pranckevičienė, I. Pundienė // Materials. — 2023. — Vol. 16, No. 14. — P. 4943. https://doi.org/10.3390/ma16144943
5.	Recovery of Mineral Wool Waste and Recycled Aggregates for Use in the Manufacturing Processes of Masonry Mortars / D. Ferrández, M. Álvarez, P. Saiz, A. Zaragoza-Benzal // Processes. — 2022. — Vol. 10, No. 5. — P. 830. https://doi.org/10.3390/pr10050830
6.	GOST 21216-2014 Clay raw materials. Test methods. — 2023.
7.	GOST 21216.1-93 Clay raw materials. Method for determination of plasticity. — 2023.
8.	Himicheskaya tehnologiya keramicheskih materialov / A.A. Крупаб V.S. Gorodov. — Kiev, Ukraine: Vishcha shkola, 2019. — 399 c.
9.	Investigation of the influence of mining waste on the properties of ceramic tiles / T.E. Shoeva // Technical Sciences: Traditions and Innovations: Proceedings of the III Intern. scientific conf. — 2018. — P. 69–72.

10. Osnovy tehnologii tugoplavkih nemetallicheskih i silikatnyh materialov / M.I. Kuzmenkov, A.A. Sakovich. — Minsk: BGTU, 2004. — 171 p.
11. Poluchenie keramicheskogo kirpicha na osnove bejdellitovoj gliny i othodov mineralnoj vaty / E.V. Vdovina. — Chelyabinsk: YuUGU, 2009. — 19 p.
12. Fiziko-himicheskie processy v keramicheskih materialah na osnove bejdellitovoj gliny i othodov proizvodstva mineralnoj vaty pri razlichnyh temperaturah obzhiga / E.V. Vdovina, V.Z. Abdrahimov // Stroitelnyj vestnik Rossijskoj inzhenernoj akademii. — 2010. — Vol. 11. — P. 47–51.
13. Use of clay bricks incorporating treated river sediments in a demonstrative building: Case study / F. El Fgaier, Z. Lafhaj, C. Chapiseau // Construction and Building Materials. — 2013. — Vol. 48. — P. 160–165. https://doi.org/10.1016/j.conbuildmat.2013.06.030
14. GOST 7025-91 Ceramic and calcium silicate bricks and stones. Methods for water absorption and density determination and frost resistance control. — 1991.
15. GOST 8462-85 Wall materials. Methods for determination of ultimate compressive and bending strength. — 1985.
16. GOST 530-2012 Ceramic brick and stone. General specifications. — 2012.

Information about authors:
Almira Kashetova – Master Student, School of Architecture, Civil Engineering and Energy, D. Serikbayev East Kazakhstan Technical University, Ust-Kamenogorsk, Kazakhstan, almira93_07@mail.ru
Aigul Kozhas – Candidate of Technical Sciences, Senior Lecturer, Department of Technology of Industrial and Civil Construction, L.N. Gumilyov Eurasian National University, Astana, Kazakhstan, kozhas@bk.ru

Author Contributions:
Almira Kashetova – concept, methodology, resources, testing, visualization, funding acquisition.
Aigul Kozhas – data collection, modeling, analysis, interpretation, drafting, editing.